Hardin, R., and Beckermann, C., "Mechanical Properties of Commercial 8630 Q&T Steel Castings: Testing Results Compared to Simulations," in Proceedings of the 76th SFSA Technical and Operating Conference, Paper No. 4.1, Steel Founders' Society of America, Chicago, IL, 2022.

Mechanical Properties of Commercial 8630 Q&T Steel Castings: Testing Results Compared to Simulations

Richard A. Hardin and Christoph Beckermann

Department of Mechanical Engineering
The University of Iowa, Iowa City, 52242

Abstract

Presented here are results of an investigation into mechanical property variations in steel castings made from 8630 quenched and tempered (Q&T) steel. Analysis of measured tensile data and casting and heat treatment processing simulation results at specimen material locations are also investigated. Mechanical properties are measured at twelve specimen locations in each of sixteen castings from four SFSA member foundries. The twelve locations are selected based on casting simulation solidification and heat treatment results to provide a range of the following simulation results and conditions; porosity volume percentage, solidification rate, the Niyama Criterion, the temperature gradient, the cooling rate, and the quench cooling rate between 800 and 500 °C (*T85*). Simulations are performed modeling process differences between the foundries, and considering differences in casting process rigging and heat treated geometry. Simulation results are exported from locations in the gage sections for the twelve specimen locations in the castings. The strength data is observed to have a strong correlation with *T85*. A significant correlation for increasing strength with increasing solidification rate is also found. Above solidification rates of 0.2 °C/s the data shows fairly consistent and high *UTS* properties, above 130 ksi. Strength estimation calculations determined from previous work using *T85* and solidification rate simulation results are compared with the measured data in the current study. The calculated strength data compare well with the measurements from this study. The standard errors of the calculations are 8.7 and 12.0 ksi for the *UTS* and *YS*, respectively, for the 153 tensile specimens tested. All strength property measurements and estimations in the present study are above the 1% lower bound strength allowable determined from a sample size of over 1560 data points from SFSA member data for cast 8630 Q&T steel. The strength estimations presented here are generally found to be conservative estimates of the strength variations in 8630 Q&T steel castings compared to the measurements.

1. Introduction

Steel castings are currently designed assuming uniform material properties and the absence of discontinuities. In order to account for possible variations in the properties and the presence of defects, large safety factors are employed leading to increased casting weight and other performance limitations. Even in the absence of discontinuities, steel castings do not have uniform properties. The property variations can be attributed to non-uniform solidification/cooling rates, quench rates and steel composition variations within a single casting as well as to process changes from casting to casting. The end goal of this investigation is the development of a simulation tool for predicting material property variations in steel castings. Such property variations can have a large impact on the performance and reliability of steel

castings. Just like the discontinuity predictions, the property variation predictions will be made part of a standard casting simulation. Ultimately the predictions can be interfaced with performance and reliability analysis tools for designing of cast steel components where the non-uniformities in the steel casting are considered.

Here the mechanical properties of commercial castings were investigated by collecting steel specimens from commercial castings, and measuring their tensile test data to determine statistically significant simulation results that correlate with mechanical properties. Approximately 190 tensile test specimens were analyzed, and these were machined from blanks cut from the same twelve locations for each casting. Altogether sixteen castings from four separate foundries were used in the study. In the case of one of the foundries three castings were produced using the same rigging system as the other foundries, and additionally three castings were produced using a naturally pressurized bottom-filled gating system. Analyses were performed as described below to correlate casting simulation results with measured mechanical properties for these commercial steel castings. A number of simulation results were found to have high statistically significant effect on the strength and ductility when correlated to the mechanical property measurements. Strength estimation equations developed in a previous study for yield and ultimate strength were applied using the simulations results in the current study. These strength estimations were found to give reasonably accurate and conservative estimates of the strength variations and inhomogeneities in 8630 Q&T steel castings.

2. Casting Process and Material Testing Procedures

The tensile test data analyzed was for specimens taken from so-called “platypus” castings because of the flat bill-like feature shown with a scaling dimension across the bill width in Figure 1(a). These were cast from an 8630 steel and a quenched and tempered heat treatment. Shown in Figure 1(a) to 1(c) are the locations of the twelve specimens that were sectioned out of the castings after heat treatment for tensile testing for all castings except one. For one of the castings, specimen blanks were first removed at the twelve specimen locations, and the blanks were heat treated. The specimens were identified as types “F” (two specimens), “H” (four specimens), and “V” (six specimens). The mechanical/tensile property measurements were performed for each specimen at an independent laboratory according to the ASTM E8-21 standard. The tensile data reported by the lab were yield strength (*YS*), ultimate strength (*UTS*), elongation (*EL*) and reduction of area (*RA*). As can be observed in Figure 1, a several specimen sizes were used in this study having gage section diameters of 0.505, 0.357 and 0.250 inches.

Except for the three castings produced by one of the foundries using a pressurized gating system, the rigging used in the casting process is shown in Figure 2. The rigging was intentionally designed to produce non-ideal or nominal filling conditions (with some splashing), and with asymmetric feeding that would result in some shrinkage porosity in the casting. This porosity would produce a range of material soundness and a resulting variation in material properties to compare with simulation results. The casting/rigging geometry heat treated by the foundries varied and these were modeled in heat treatment simulations using the *MAGMAsteel* module in the software *MAGMAsoft*. In some cases, the rigging was not removed before the casting was heat treated. For example, in Figure 3(a) a platypus casting heat treated with the full

rigging attached is shown. The simulation result shown in Figure 3 is the quench cooling rate between 800 °C and 500 °C (*T85*). In other cases the castings are heat treated with only easy to remove feeder sections removed as shown in Figure 3(b), or the entire rigging was removed as shown in Figure 3(c). Accordingly, one of the geometries shown in Figure 3 was used in simulations of the heat treatment process.

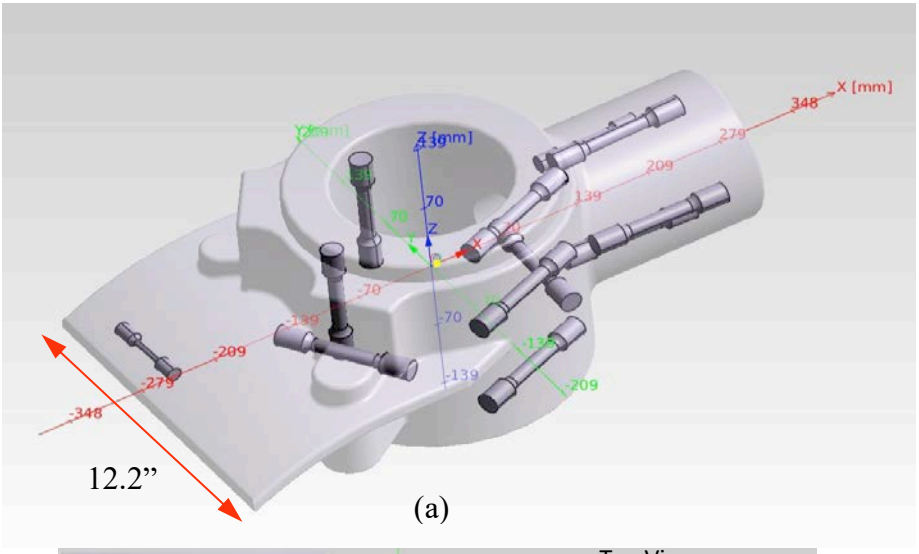

(a)

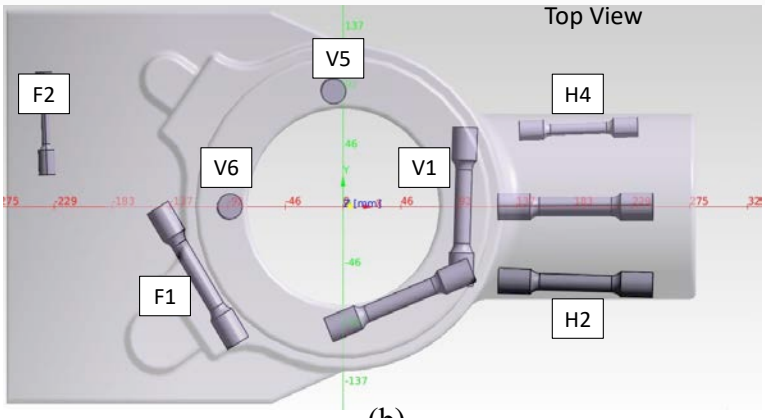

(b)

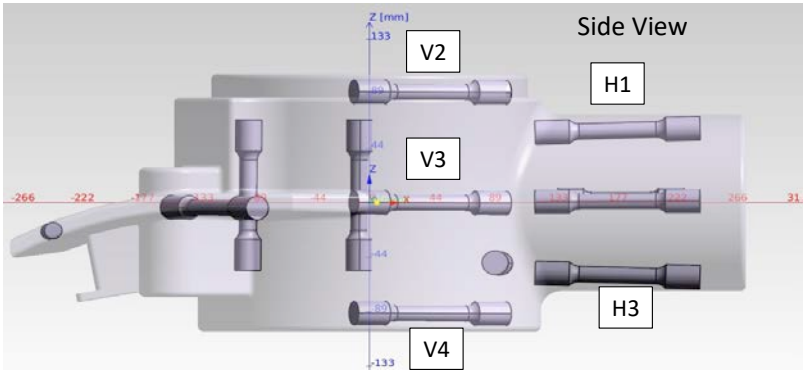

(c)

Figure 1 Views (a), (b), and (c) in an x-ray format of the locations of the twelve specimens sectioned out of the platypus castings after heat treatment for tensile testing.

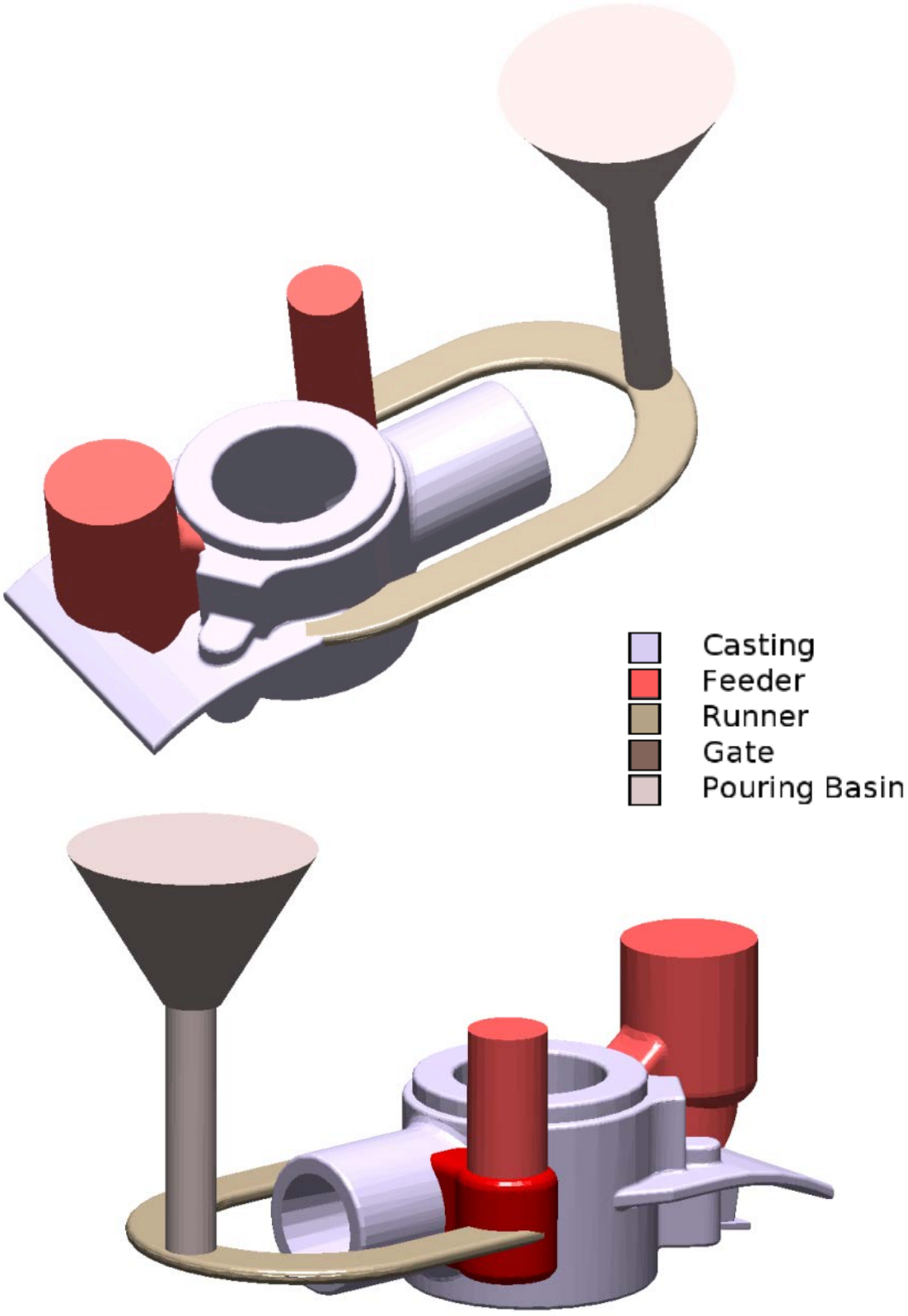

Figure 2 The rigging used in the casting process for thirteen of the castings used in the study. The remaining three castings were produced using a pressurized gating system by one of the foundries.

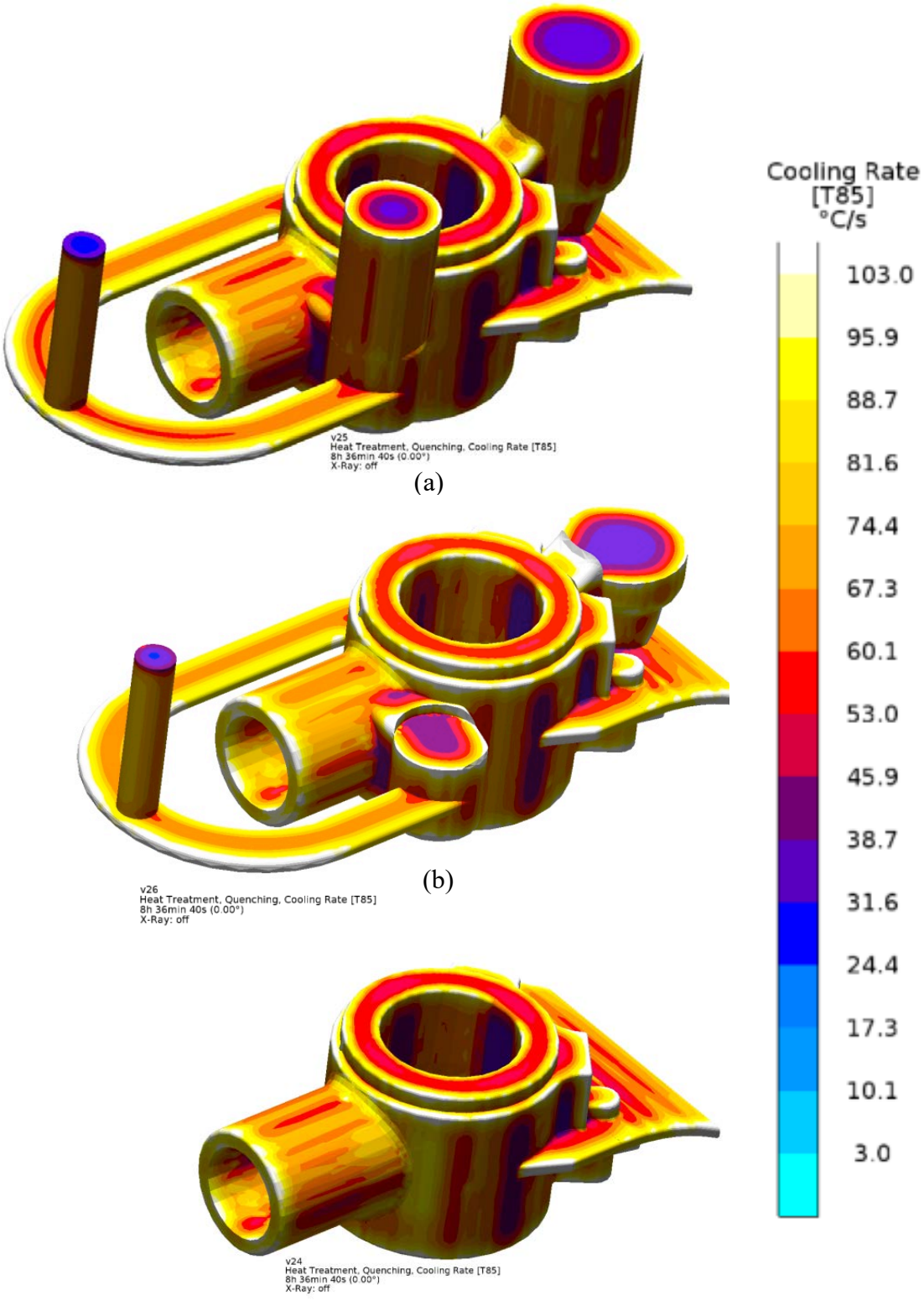

Figure 3 The quench cooling rate between 800 °C and 500 °C (*T85*) results for the platypus casting heat treated with the full rigging still attached (a), heat treated with the feeders removed (b), and heat treated with the rigging removed (c).

3. Simulation and Analysis Procedures

The software *MAGMAsoft* [1] was used to simulate the filling and solidification processes of all castings discussed here. Its *MAGMAsteel* module was used to simulate the heat treatment processes. The tensile specimens were taken from the castings at prescribed locations such that a range of solidification and microstructural conditions would result at the specimen locations. To accurately extract the results of the simulation results, models of the specimens were included in the simulation models at their locations as shown in Figure 1. The test specimen blanks were cut from the castings at the locations with as much accuracy as possible by our colleagues either at the participating Steel Founders' Society (SFSA) member foundries or at the University of Alabama-Birmingham (UAB). The solid models of each casting and its specimens were assembled, and these were provided for all castings to the foundries and UAB to communicate the specimen locations in the castings as accurately as possible.

The simulation results identified to have statistical significance to properties over the course of this project are the porosity volume percentage, solidification rate (over full solidification temperature range), the Niyama Criterion (a thermal-based predictor of porosity), the temperature gradient used in Niyama Criterion, the cooling rate used in Niyama Criterion (it ignores first and last 10% of solidification) and the cooling rate between 800 °C and 500 °C during the quenching process (referred to as *T85*). The representative simulation results in the specimen gage sections were determined by using a feature in the software postprocessor to select points in the simulation model and export the simulation results at those locations for analysis. Data is collected from the gage sections of the specimen locations using this feature of the *MAGMAsoft* results postprocessor at ten points to determine a mean and the variation. As shown in Figure 4 ten points are selected in the specimen gage section. Points are selected to capture the minimum and maximum values, and at eight representative values at well-spaced

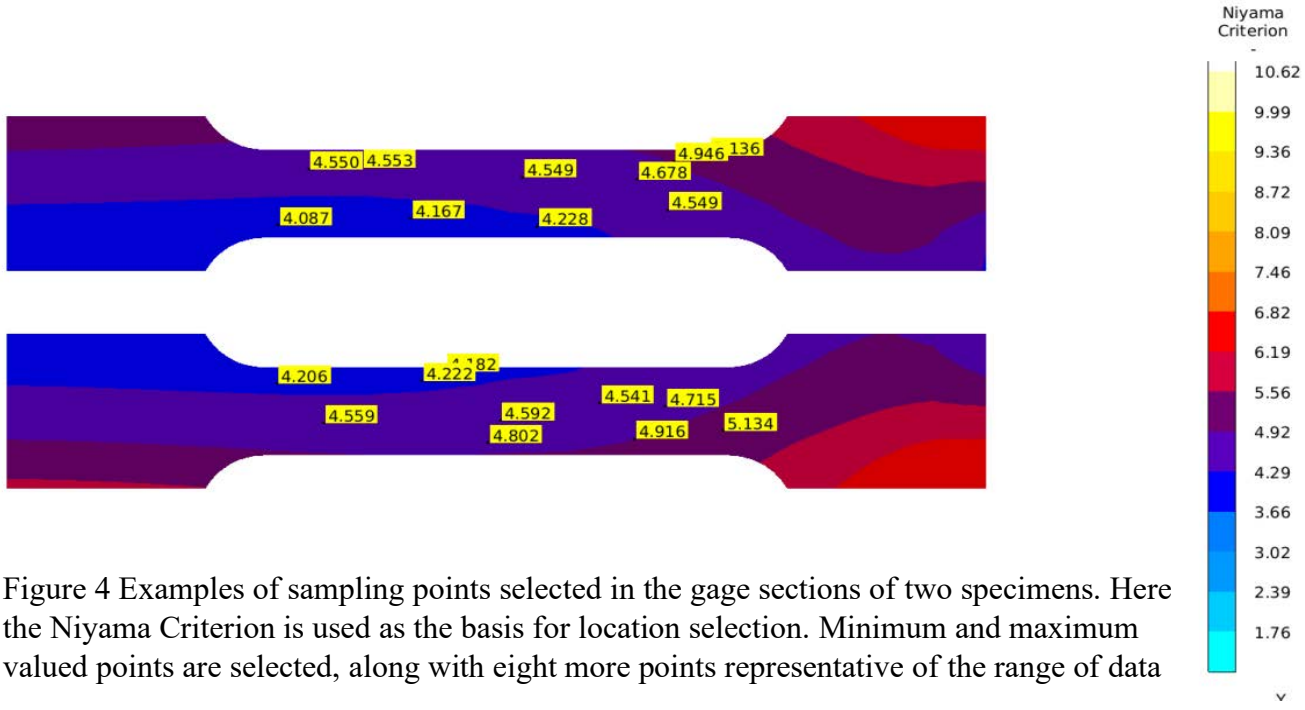

Figure 4 Examples of sampling points selected in the gage sections of two specimens. Here the Niyama Criterion is used as the basis for location selection. Minimum and maximum valued points are selected, along with eight more points representative of the range of data

points. The ten values for all simulation results for each specimen are exported to a spreadsheet, and the mean and standard deviation are calculated for plotting the representative value and its variation.

Simulation Description

The casting simulation conditions are described below so readers use them in their own applications of the results from this study. The casting process simulations were performed using general solidification parameters given in Table 1. Also given in the table is the chemistry used in the heat treatment simulations. Temperature dependent solid fraction-temperature curve (solidification curve) and thermophysical properties are given in Figures 5 to 7. The pouring temperature used in the simulations was 2912 °F (1600°C), and the filling time was 8.5 seconds. The software's database properties used for the mold was no-bake silica sand (cold box silica). Heat transfer coefficients used between the steel and mold were defined by a temperature dependent curve having a value of 1000 W/m^2-K above 1600°C, ramping down at a constant rate to 100 W/m^2-K at 1000°C, and was then a constant 100 W/m^2-K at lower temperatures. Between all other materials a constant 800 W/m^2-K heat transfer coefficient was used.

Table 1 General solidification parameters and chemistry used in solidification and heat treatment simulations.

Solidus temperature	1425.00	°C
Liquidus temperature	1502.00	°C
Niyama Criterion Temperature	1432.70	°C
Thermo Criteria Temperature	1504.00	°C
Initial temperature	1600.00	°C
Latent heat	251.0000	kJ/kg

Carbon	0.3000	%
Silicon	0.2500	%
Manganese	0.8000	%
Phosphorus	0.0200	%
Sulfur	0.0200	%
Aluminium	0.0000	%
Cobalt	0.0000	%
Chromium	0.5000	%
Copper	0.0000	%
Molybdenum	0.2000	%
Nickel	0.5500	%
Titanium	0.0000	%
Vanadium	0.0000	%
Tungsten	0.0000	%

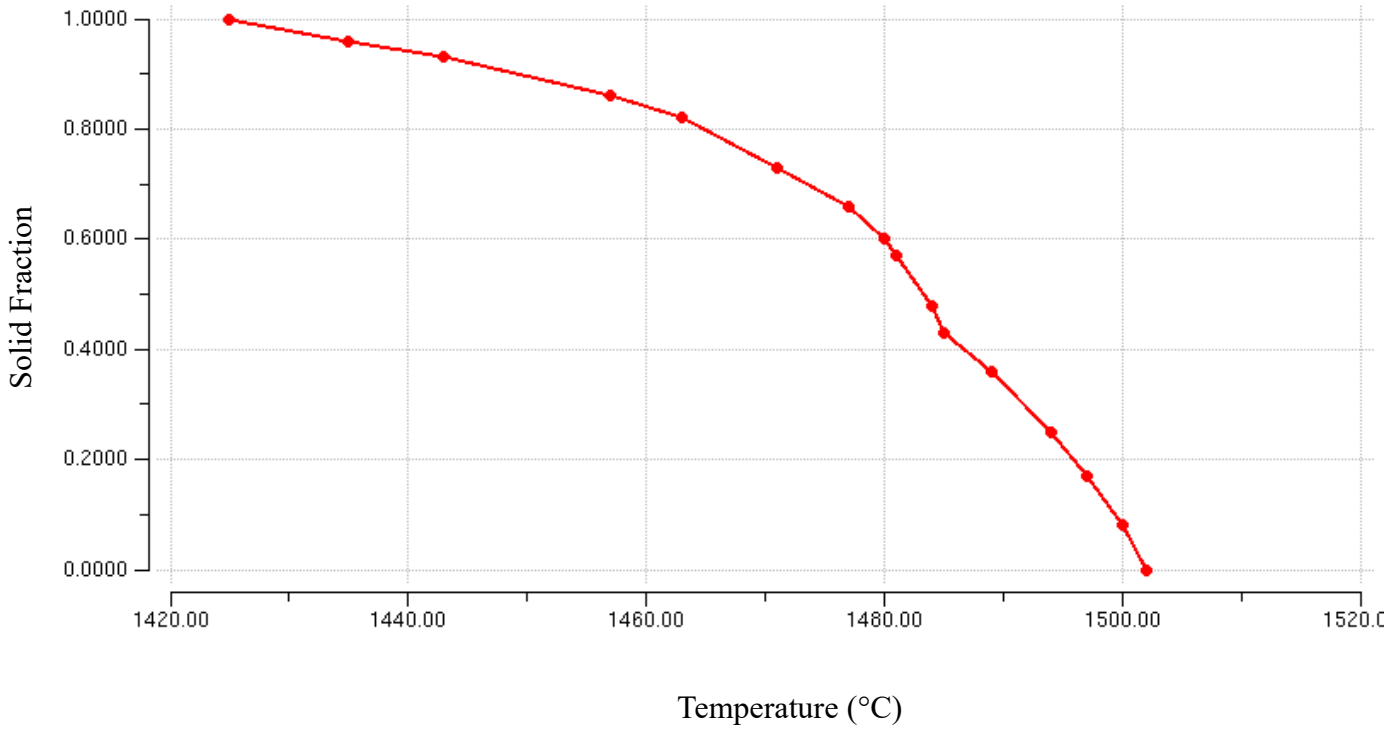

Figure 5 Solid fraction-temperature curve (solidification curve) for the 8630 Q&T alloy. The liquidus temperature is 1502 °C (2735 °F) and solidus temperature is 1425 °C (2597 °F).

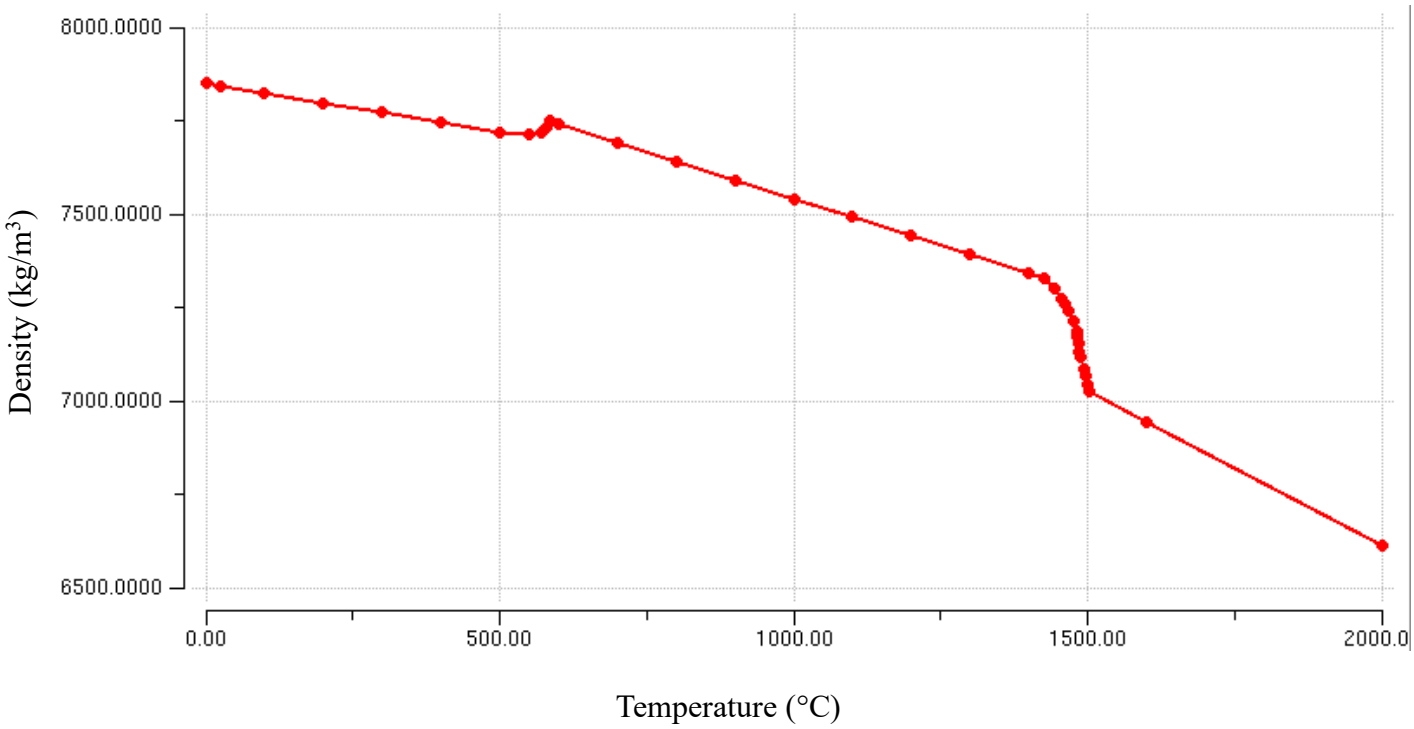

Figure 6 Temperature dependent density used in simulations for the 8630 alloy.

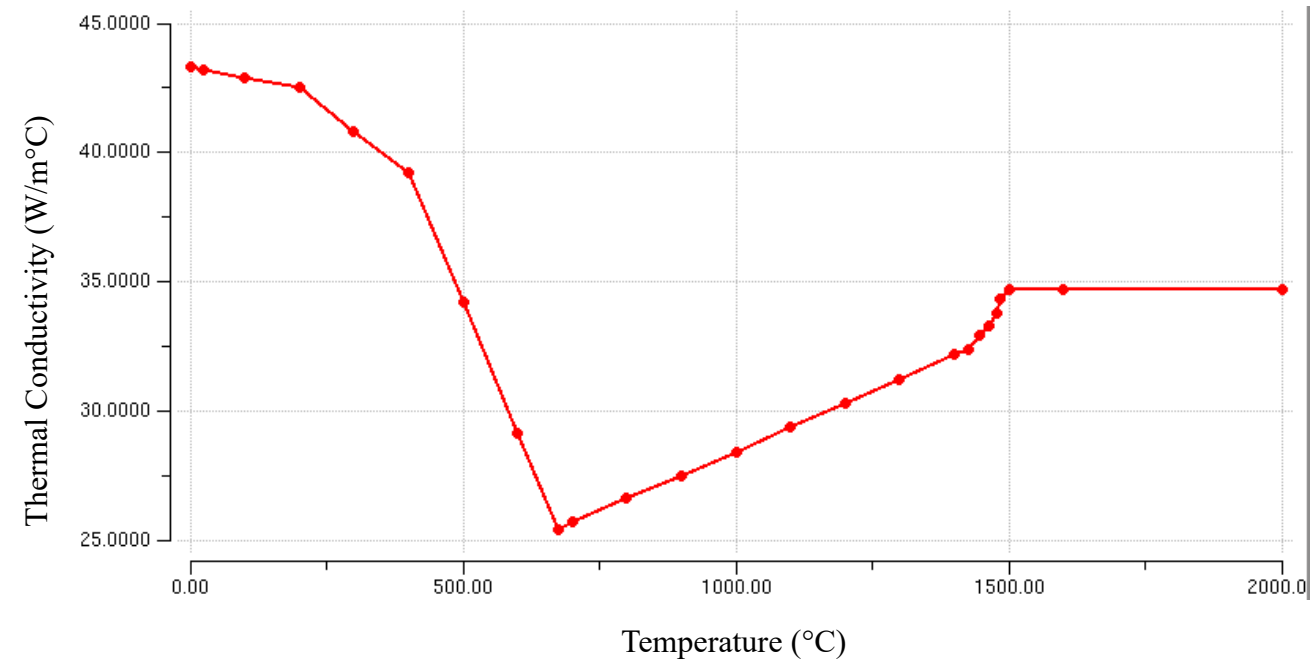

(a)

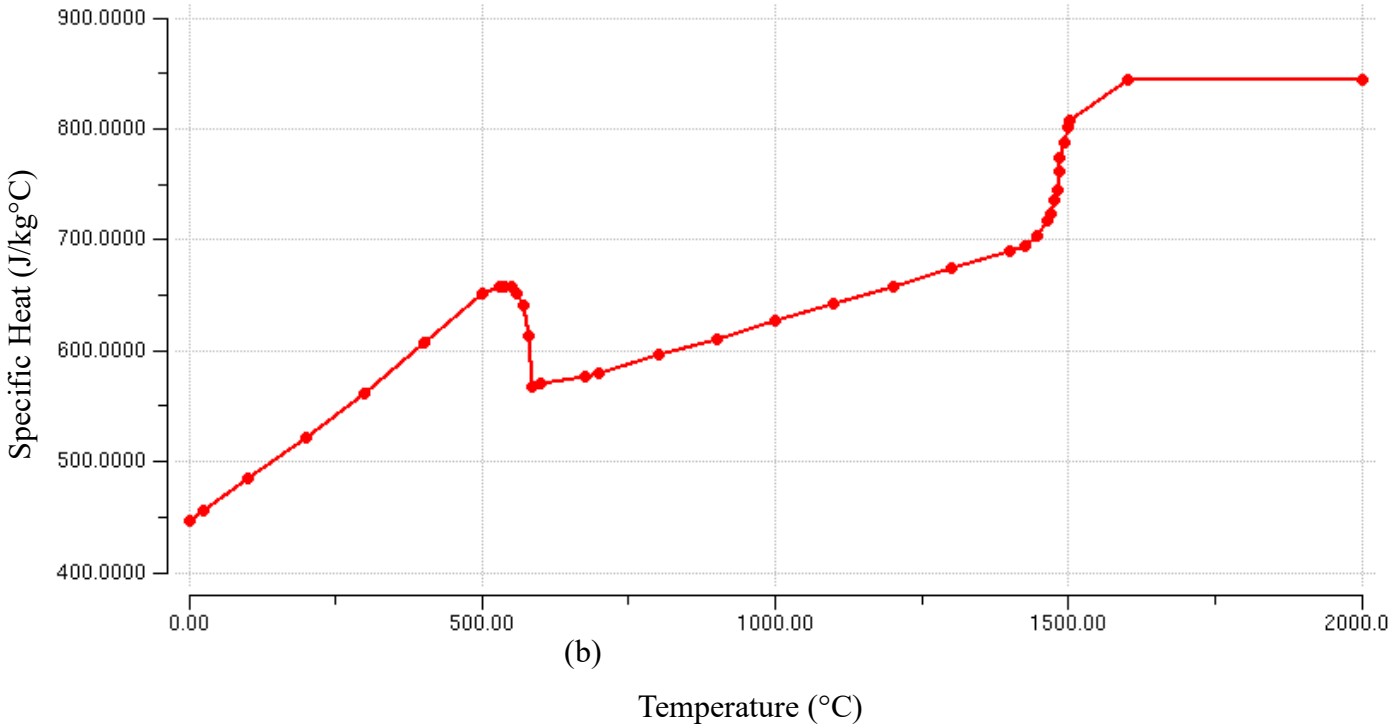

(b)

Figure 7 Temperature dependent properties used in simulations for the 8630 alloy for (a) Thermal conductivity, (b) specific heat.

4. Tensile Properties and Simulation Results

This section reports on the measured mechanical properties and their variation. The variation between the foundries is presented. The variation of the measured data by specimen location in the castings is analyzed and presented as well.

As mentioned in the introduction, sixteen castings from four foundries were produced for the study with twelve tensile test specimens tested from each casting. One of the four foundries produced three castings using the same rigging system as the other foundries (shown in Figure 2), and also another three castings produced using a naturally pressurized bottom-filled gating system (not shown here). In the interest of anonymity, the capital letters V, W, X, Y and Z will be used to identify the foundry and gating system used to produce the castings for a given group of test specimens. The foundry and gating system identifiers (V through Z) will be referred in short as “foundry IDs” or as “foundries”. The measured tensile properties for all foundries are given by specimen ID and grouped by casting in Tables 1 through 6 along with specimen size tested and summary statistics. The statistical analyses and results presented in this paper were performed using *Minitab* [2] and *SAS* [3] software. All specimen material was sectioned out of the castings after heat treatment for tensile testing except for one. For one of the foundry W castings, the specimen blanks were first removed at the twelve specimen locations, and then the blanks were heat treated. This data is given in Table 3, and the uniformly high quench effect for these specimens produces uniformly high strength properties. The tables of data are provided to share the detail with the SFSA membership. Note that tensile data is missing for three specimens as the test result did not conform to the standard.

Histogram plots of the tensile property data along with calculated normal distributions are given in Figure 8 for the strength measurements and in Figure 9 for the ductility data. The histogram plots also include the mean, standard deviation and number of specimens. Note that generally the distributions of data shown by the histograms do not appear to follow a normal distribution. This is not surprising as the data is not a product of random sampling. Box plots of the tensile test measurements are given by foundry ID in Figures 10 and 11, for the strength and ductility data, respectively. The elements of the box plots are defined in Figure 10(a). These are; means connected by lines, end of the boxes denote the range, horizontal line is the median, symbols indicate outliers, and the smaller inner boxes denotes the interquartile range (50% of the data distribution). The whisker lines extending from the interquartile range box give the top and bottom 25% of data values excluding outliers. Looking at the strength data in Figure 10 it is apparent that the data for foundry X lies outside and lower than all the other foundries. The *UTS* data is nearly outside the ranges of all the other foundries. The ductility data in Figure 11 for foundry X is higher than but not outside the ranges of the other foundries. In general for the rest of this paper, the foundry X data will be excluded from analysis of the mechanical property data. The reason for the reduced strength data from foundry X could not be establish at the time of the writing of this paper. Histograms for the strength and ductility data with the foundry “X” data removed are given in Figures 12 and 13, respectively. Without the foundry X data, the standard deviation for the strength data is reduced by about 3 ksi, and there is not a great change in the ductility data variation.

Table 1 Tensile test data for 36 specimens from three castings from Foundry V.

Specimen Location ID	Diameter (in)	UTS (ksi)	YTS (ksi)	Elongation (%)	RA (%)
F1	0.505	123.0	101.4	4	10
F2	0.25	150.0	139.2	12	33
H1	0.505	142.4	129.5	10	24
H2	0.505	140.7	128.0	11	27
H3	0.505	137.9	124.9	10	25
H4	0.357	137.9	126.0	11	29
V1	0.505	135.4	121.2	6	16
V2	0.505	142.4	127.8	13	40
V3	0.505	127.0	112.1	3	8
V4	0.505	136.4	120.8	15	38
V5	0.505	123.9	106.7	5	14
V6	0.505	127.0	104.3	6	15
F1	0.357	123.9	108.8	4	14
F2	0.25	148.8	138.2	11	31
H1	0.505	143.3	130.4	10	29
H2	0.505	144.4	133.1	8	18
H3	0.505	142.2	130.4	9	25
H4	0.357	140.2	128.3	10	26
V1	0.505	135.7	121.3	3	15
V2	0.505	141.7	126.5	14	37
V3	0.505	126.1	107.6	5	15
V4	0.505	135.5	116.2	13	36
V5	0.505	124.6	108.2	3	9
V6	0.505	124.0	101.0	5	11
F1	0.357	122.4	101.9	10	24
F2	0.25	136.4	124.7	12	31
H1	0.505	142.5	128.4	11	25
H2	0.505	145.8	133.8	11	24
H3	0.505	144.0	131.7	9	16
H4	0.357	137.0	122.5	10	31
V1	0.505	133.9	121.5	5	10
V2	0.505	142.2	128.7	13	26
V3	0.505	124.6	104.9	8	15
V4	0.505	137.5	122.5	13	34
V5	0.505	121.7	102.5	7	17
V6	0.505	111.8	104.7	4	9
Average	------>	134.8	120.0	8.6	22.4
Stdev	------>	9.2	11.6	3.6	9.4
Number	------>	36.0	36.0	36.0	36.0
95% Mean	------>	3.0	3.8	1.2	3.1
Max	------>	150.0	139.2	15.0	40.0
Min	------>	111.8	101.0	2.5	7.5

Table 2 Tensile test data for 36 specimens from three castings for Foundry W.

Specimen Location ID	Diameter (in)	UTS (ksi)	YTS (ksi)	Elongation (%)	RA (%)
F1	0.357	126.7	104.3	11	26
F2	0.25	144.9	132.1	12	31
H1	0.505	136.1	122.2	11	28
H2	0.505	137.2	122.1	10	25
H3	0.505	137.1	122.2	10	23
H4	0.357	134.5	120.1	11	28
V1	0.505	134.2	117.3	8	16
V2	0.505	137.9	121.9	14	36
V3	0.505	125.1	106.1	9	17
V4	0.505	132.2	114.6	14	38
V5	0.505	123.9	107.5	4	13
V6	0.505	125.9	103.8	9	17
F1	0.357	121.8	99.5	8	17
F2	0.25	145.0	131.9	12	41
H1	0.505	136.7	122.4	12	18
H2	0.505	136.6	121.5	10	18
H3	0.505	136.1	121.0	13	31
H4	0.357	134.5	120.6	11	30
V1	0.505	130.2	116.9	7	12
V2	0.505	140.0	123.8	12	27
V3	0.505	123.7	104.3	10	19
V4	0.505	132.0	115.5	13	37
V5	0.505	115.2	105.7	3	9
V6	0.505	124.3	102.1	8	13
F1	0.357	113.2	92.0	11	30
F2	0.25	130.5	114.6	16	49
H1	0.505	137.4	122.8	12	29
H2	0.505	136.0	121.1	11	25
H3	0.505	136.5	121.2	12	25
H4	0.357	134.4	120.5	12	36
V1	0.505	133.3	116.3	13	33
V2	0.505	134.4	117.7	16	38
V3	0.505	123.7	105.1	8	22
V4	0.505	128.0	110.4	14	34
V5	0.505	118.9	97.9	12	29
V6	0.505	115.7	93.3	10	15
Average	------>	130.9	114.2	10.7	26.0
Stdev	------>	7.9	10.2	2.9	9.4
Number	------>	36.0	36.0	36.0	36.0
95% Mean	------>	2.6	3.3	0.9	3.1
Max	------>	145.0	132.1	16.0	49.0
Min	------>	113.2	92.0	3.0	9.0

Table 3 Tensile test data for specimens from one casting for Foundry W, where specimen blanks were removed from the casting before being quenched and tempered.

Specimen Location ID	Diameter (in)	UTS (ksi)	YTS (ksi)	Elongation (%)	RA (%)
F1	0.357	141.2	127.3	15	19
F2	0.25	141.1	126.6	16	45
H1	0.357	141.4	128.0	11	22
H2	0.357	141.2	127.8	13	16
H3	0.357	142.1	128.8	11	18
H4	0.25	141.9	128.1	14	25
V1	0.505	140.9	127.9	8	15
V2	0.357	142.9	129.0	16	32
V3	0.357	139.6	126.9	8	9
V4	0.505	139.9	126.5	14	38
V5	0.357	133.3	124.8	6	8
V6	0.505	137.6	127.2	5	6
Average	------>	140.3	127.4	11.3	21.0
Stdev	------>	2.6	1.1	4.0	12.2
Number	------>	12.0	12.0	12.0	12.0
95% Mean	------>	1.5	0.6	2.3	6.9
Max	------>	142.9	129.0	16.0	45.0
Min	------>	133.3	124.8	5.0	5.5

Table 4 Tensile test data for specimens from three castings for Foundry X

Specimen Location ID	Diameter (in)	UTS (ksi)	YTS (ksi)	Elongation (%)	RA (%)
F1	0.505	107.7	86.7	18	42
F2	0.25	114.6	94.2	19	48
H1	0.505	114.8	95.8	19	42
H2	0.505	112.3	92.1	19	39
H3	0.505	114.1	94.5	17	30
H4	0.357	116.3	97.2	19	48
V1	0.505	112.2	96.6	13	23
V2	0.505	116.0	98.2	21	55
V3	0.505	101.9	78.3	20	50
V4	0.505	109.6	89.3	23	59
V5	0.505	105.8	83.8	11	14
V6	0.505	104.0	87.0	11	25
F1	0.502	100.2	74.6	23	44
F2	0.2521	115.3	96.1	21	51
H1	0.5032	114.6	95.2	19	45
H2	0.5023	113.3	93.7	17	37
H3	0.5009	113.0	94.2	19	45
H4	0.3518	112.9	93.0	21	52
V1	0.5015	109.3	92.7	15	33
V2	0.5009	114.3	94.1	22	53
V3	0.5036	106.0	83.3	19	42
V4	0.502	112.0	92.1	23	57
V5	0.2528	104.4	81.1	18	22
V6	0.5022	104.0	81.7	13	23
F1	0.5014	99.2	73.2	24	53
F2	0.2528	114.2	94.9	20	48
H1	0.5033	114.1	94.5	19	40
H2	0.5023	114.7	95.2	19	45
H3	0.5022	112.3	92.6	17	36
H4	0.351	111.4	90.7	21	50
V1	0.5013	112.2	92.5	16	37
V2	0.5016	115.5	95.9	21	47
V3	0.5019	108.2	86.3	17	27
V4	0.5022	111.1	91.0	24	59
V5	0.5032	102.1	79.8	14	23
V6	0.5019	103.2	83.0	8	18
Average	------>	110.2	89.9	18.3	40.6
Stdev	------>	5.0	6.7	3.8	12.3
Number	------>	36.0	36.0	36.0	36.0
95% Mean	------>	1.6	2.2	1.2	4.0
Max	------>	116.3	98.2	24.0	59.0
Min	------>	99.2	73.2	8.0	14.0

Table 5 Tensile test data for 36 specimens from three castings from Foundry Y

Specimen Location ID	Diameter (in)	UTS (ksi)	YTS (ksi)	Elongation (%)	RA (%)
F1	0.357	119.9	100.6	11	26
F2	0.25	137.1	123.6	16	32
H1	0.505	137.6	125.5	15	40
H2	0.505	137.3	123.5	13	33
H3	0.505				
H4	0.357	137.5	127.0	16	40
V1	0.505	137.5	125.0	11	14
V2	0.505	137.4	124.8	14	37
V3	0.505	129.1	115.1	8	14
V4	0.505	136.5	123.4	15	37
V5	0.505	128.8	115.4	6	8
V6	0.505	124.8	107.2	10	22
F1	0.505	123.1	105.0	9	15
F2	0.25	135.3	121.2	16	38
H1	0.505	135.5	122.6	14	30
H2	0.505	135.6	122.5	12	20
H3	0.505	136.8	122.9	14	40
H4	0.357	135.7	124.5	16	31
V1	0.505	135.5	122.7	15	40
V2	0.505	136.1	124.1	17	50
V3	0.505	131.6	117.2	12	26
V4	0.505	135.0	121.9	18	47
V5	0.505	119.4	114.0	4	10
V6	0.505	113.1	104.4	4	14
F1	0.357	129.8	113.9	11	26
F2	0.25	139.8	127.4	15	40
H1	0.505	138.3	126.5	14	30
H2	0.505	138.1	126.2	14	23
H3	0.505	138.9	127.4	12	27
H4	0.357	138.7	127.4	16	38
V1	0.505	140.0	128.6	15	40
V2	0.505	139.2	128.4	16	43
V3	0.505	135.2	122.9	11	19
V4	0.505	138.8	127.5	13	28
V5	0.505	127.4	111.8	11	20
V6	0.505	130.9	115.5	12	23
Average	------>	133.5	120.5	12.7	29.2
Stdev	------>	6.6	7.5	3.5	11.0
Number	------>	35.0	35.0	35.0	35.0
95% Mean	------>	2.2	2.5	1.2	3.6
Max	------>	140.0	128.6	18.0	50.0
Min	------>	113.1	100.6	4.0	7.5

Table 6 Tensile test data for 36 specimens from three castings from Foundry Z.

Specimen Location ID	Diameter (in)	UTS (ksi)	YTS (ksi)	Elongation (%)	RA (%)
F1	0.505	119.1	92.7	16	24
F2	0.25	141.2	126.7	13	31
H1	0.505	138.3	123.2	9	14
H2	0.505	138.6	124.0	10	17
H3	0.505	138.8	124.0	12	25
H4	0.357	132.3	113.5	14	42
V1	0.505	127.4	109.7	5	7
V2	0.505	126.0	109.7	5	7
V3	0.505	123.9	99.5	12	20
V4	0.505	130.8	111.6	16	35
V5	0.505	123.7	100.5	10	13
V6	0.505	116.8	91.1	12	20
F1	0.5016	115.6	94.4	7	11
F2	0.2525	140.6	125.0	15	18
H1	0.5017	134.5	122.8	6	14
H2	0.5013	139.8	123.7	13	29
H3	0.5019	139.7	124.2	13	27
H4	0.3538	133.8	114.3	15	40
V1	0.5011	133.4	113.9	15	29
V2	0.502	128.8	111.2	7	10
V3	0.5014	125.4	100.5	11	23
V4	0.5008	130.9	108.2	17	44
V5	0.502	123.4	97.7	13	27
V6	0.501	118.0	92.8	14	32
F1	0.5017	114.8	85.4	15	38
F2	0.2528	139.8	124.2	13	34
H1	0.5007	136.4	119.0	10	23
H2	0.505				
H3	0.3523	137.5	121.4	10	17
H4	0.3527	129.0	107.5	15	36
V1	0.5015	123.4	108.0	5	14
V2	0.5022	133.8	114.2	9	6
V3	0.505				
V4	0.5023	132.4	111.0	18	43
V5	0.5005	120.9	95.4	8	11
V6	0.5021	116.8	91.2	13	26
Average	------>	129.6	109.8	11.6	23.7
Stdev	------>	8.3	12.2	3.7	11.2
Number	------>	34.0	34.0	34.0	34.0
95% Mean	------>	2.8	4.1	1.2	3.8
Max	------>	141.2	126.7	18.0	44.0
Min	------>	114.8	85.4	5.0	6.0

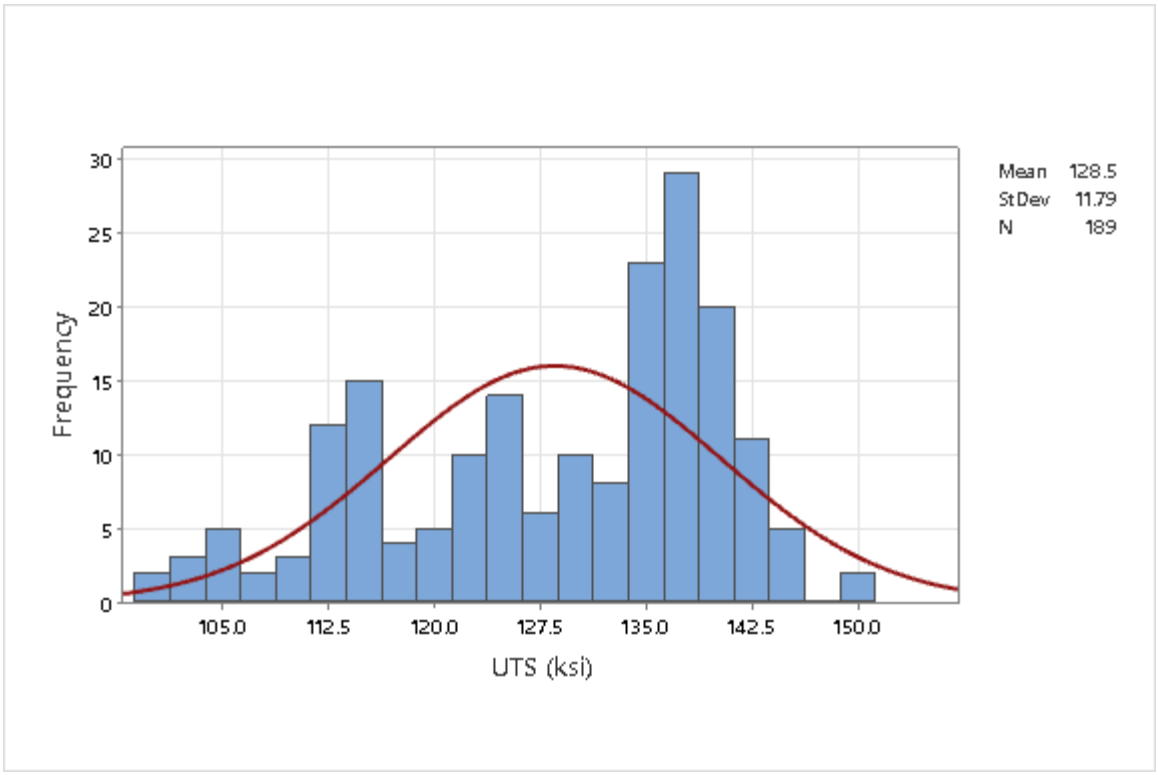

(a)

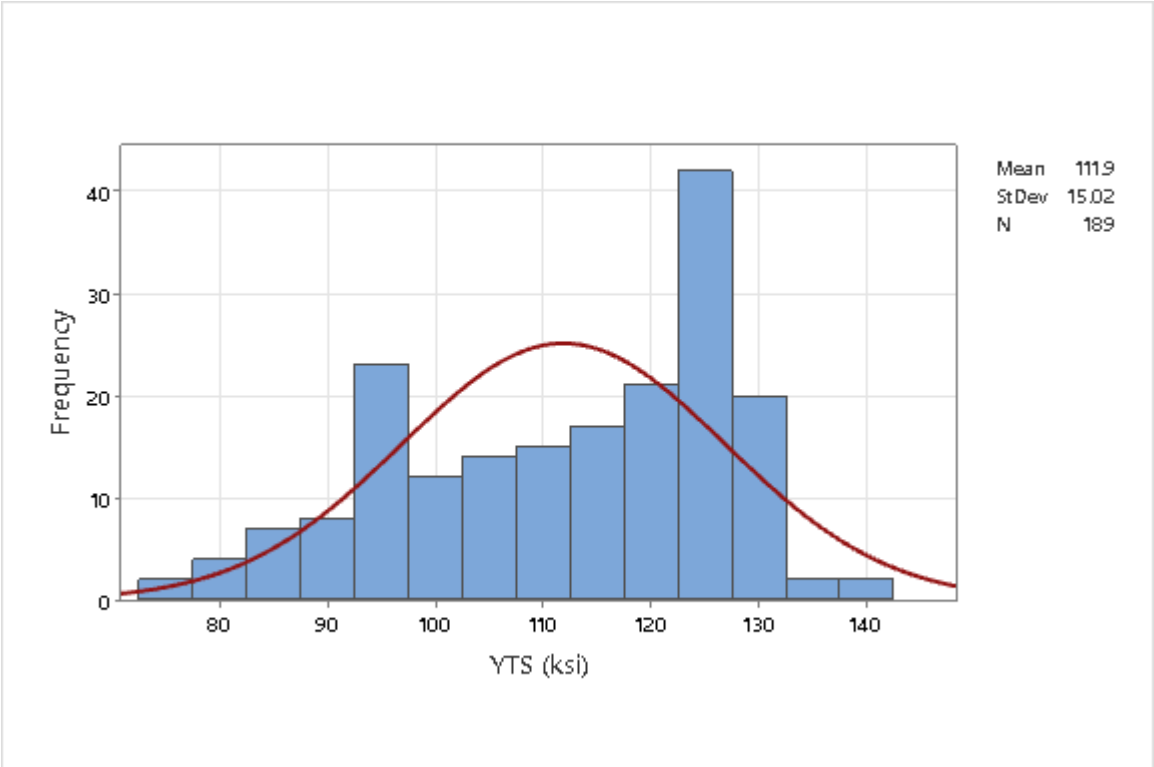

(b)

Figure 8 Histograms for all strength data with UTS data shown in (a) and yield strength data shown in (b).

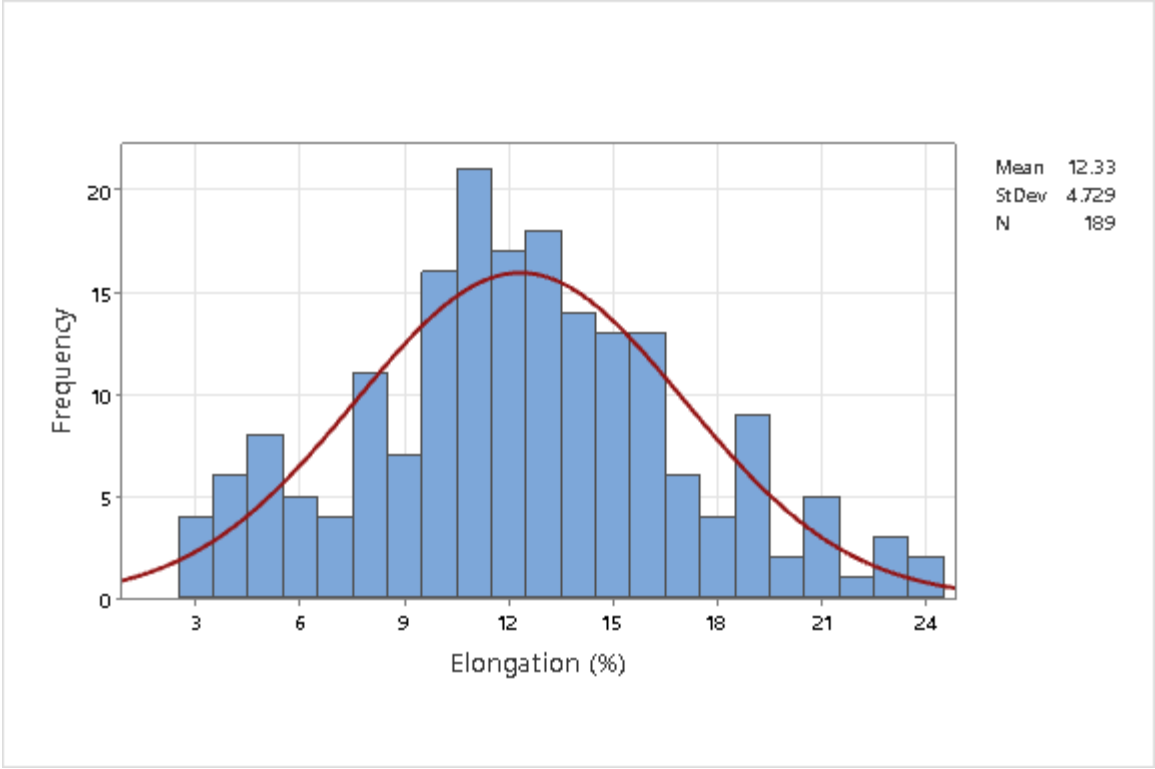

(a)

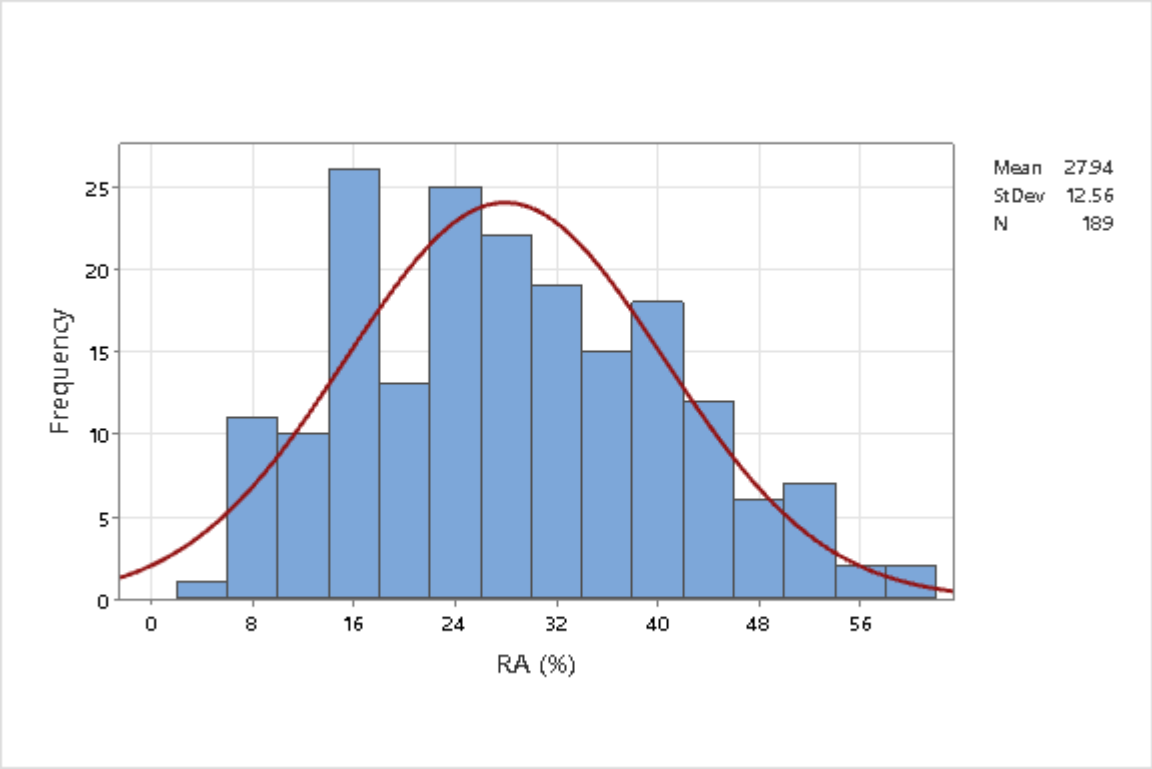

(b)

Figure 9 Histograms for all ductility data with elongation data shown in (a) and reduction of area data shown in (b).

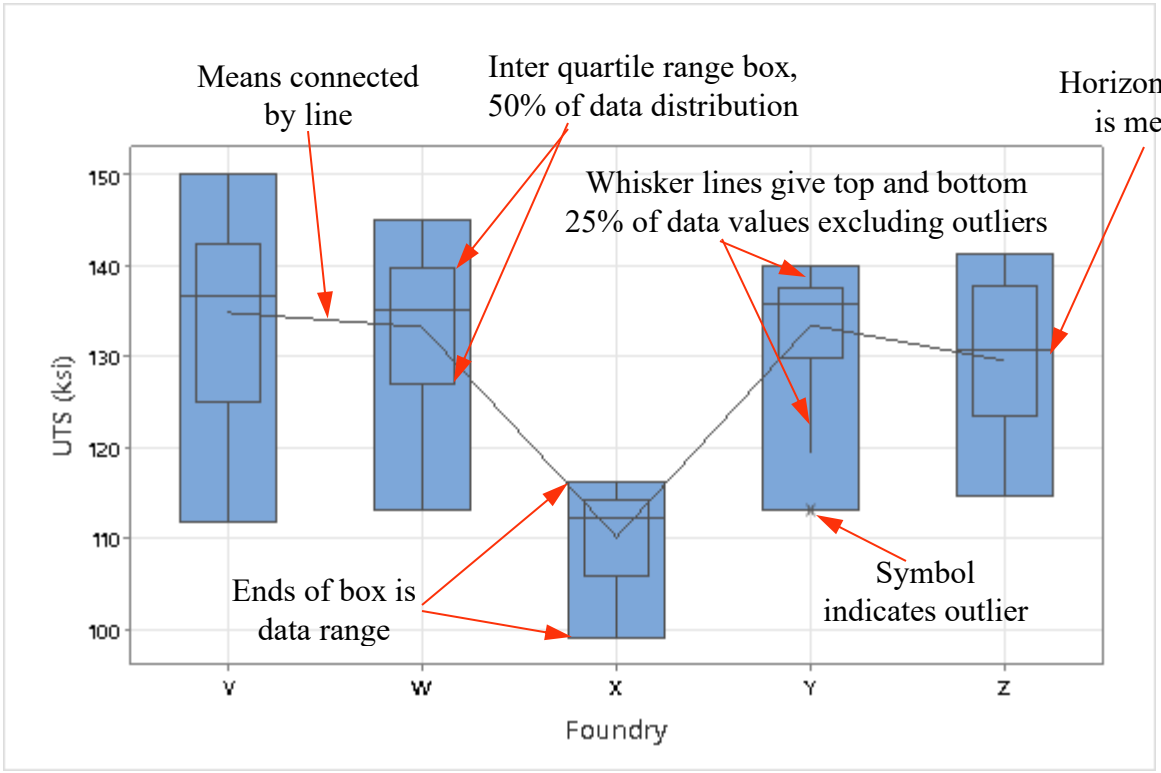

(a)

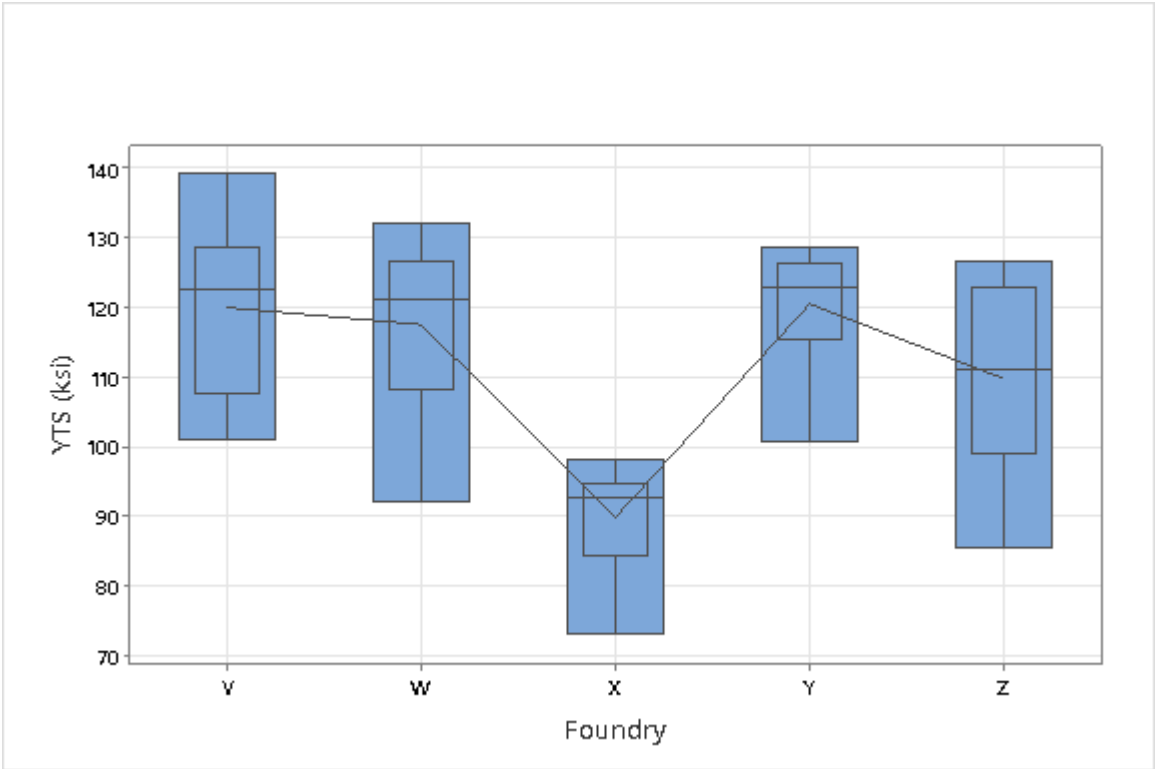

(b)

Figure 10 Box plots for strength data analyzed by foundry/process. UTS data shown in (a) also gives the definitions of the box plot elements. Yield strength data shown in (b).

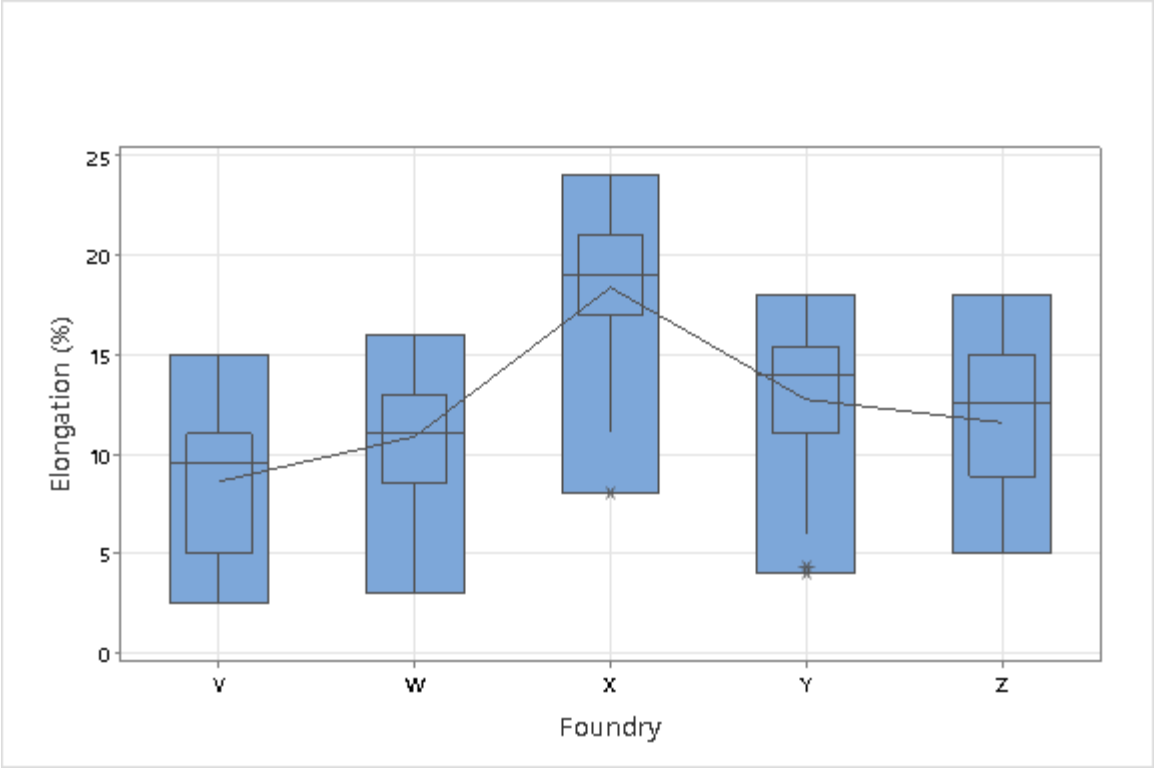

(a)

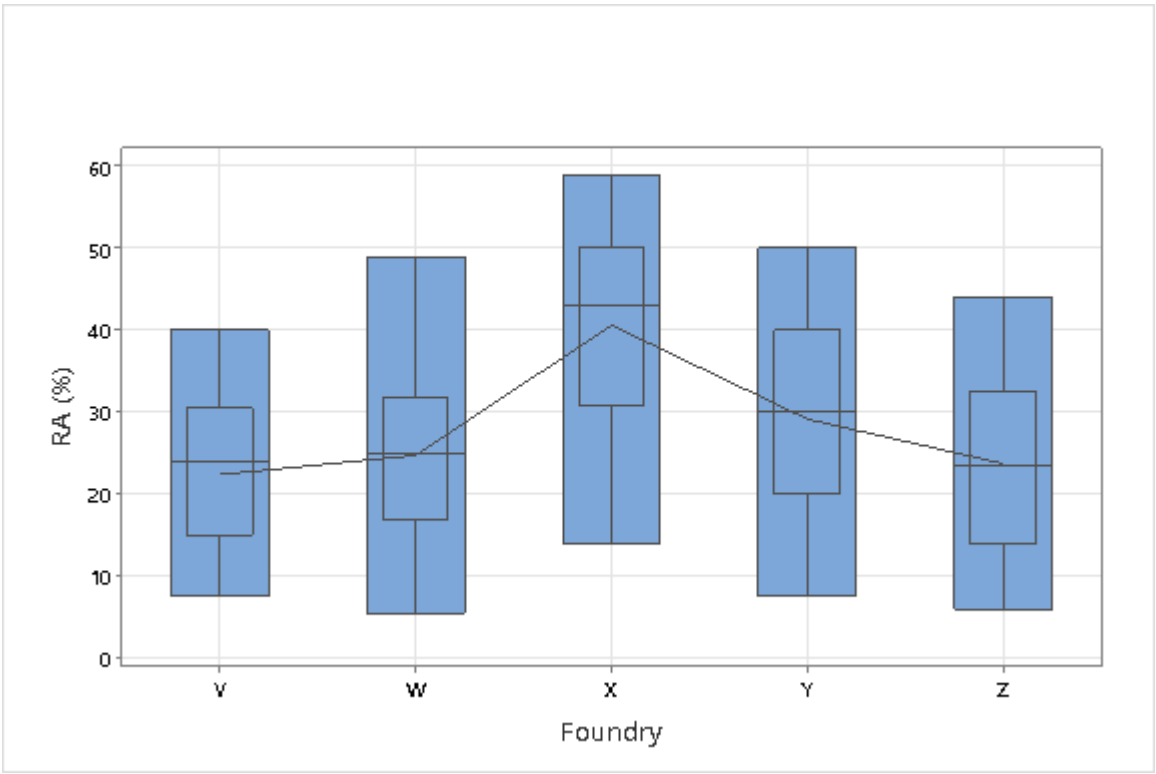

(b)

Figure 11 Box plots for ductility data analyzed by foundry/process. Elongation data shown in (a) and reduction of area data is shown in (b).

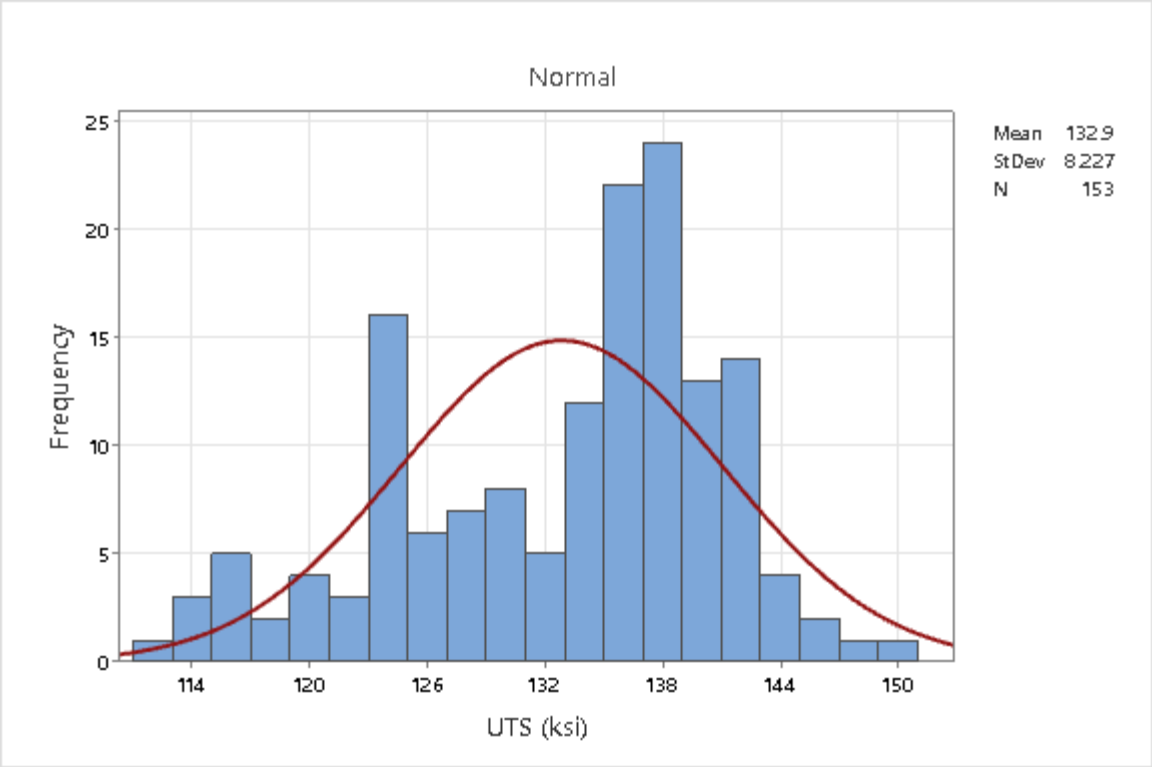

(a)

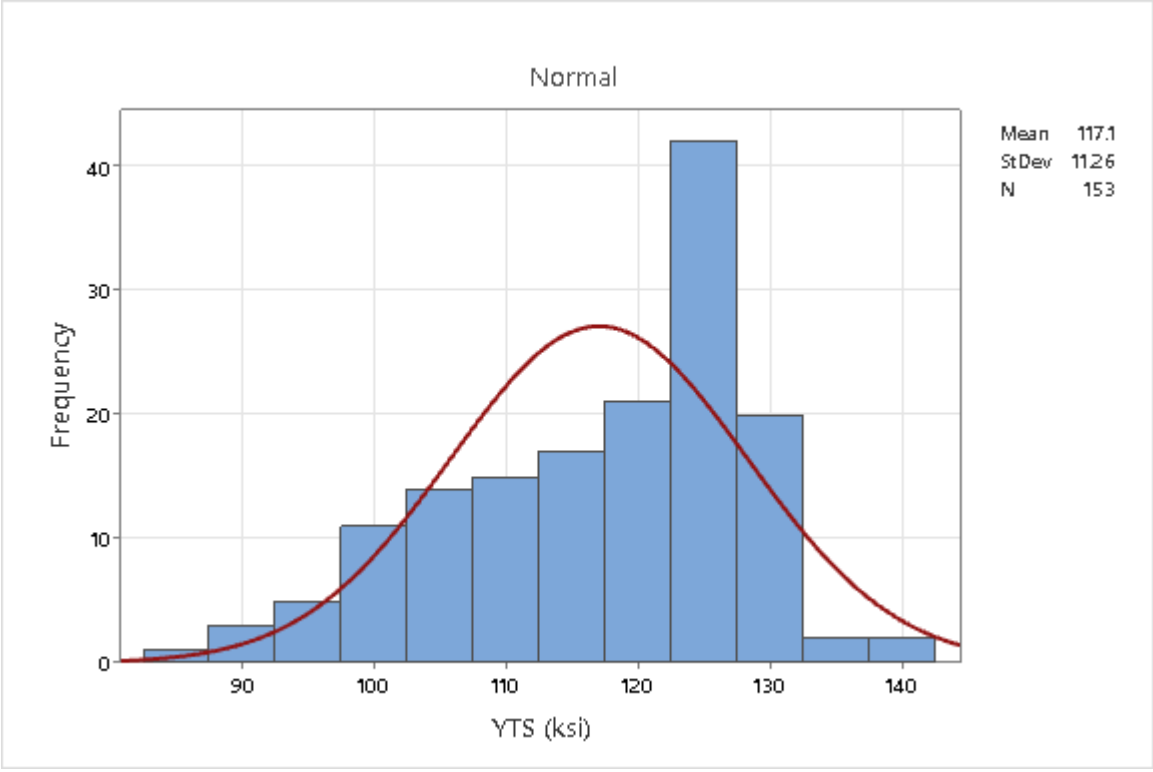

(b)

Figure 12 Histograms for strength with foundry "X" data removed. UTS data is shown in (a) and yield strength data shown in (b).

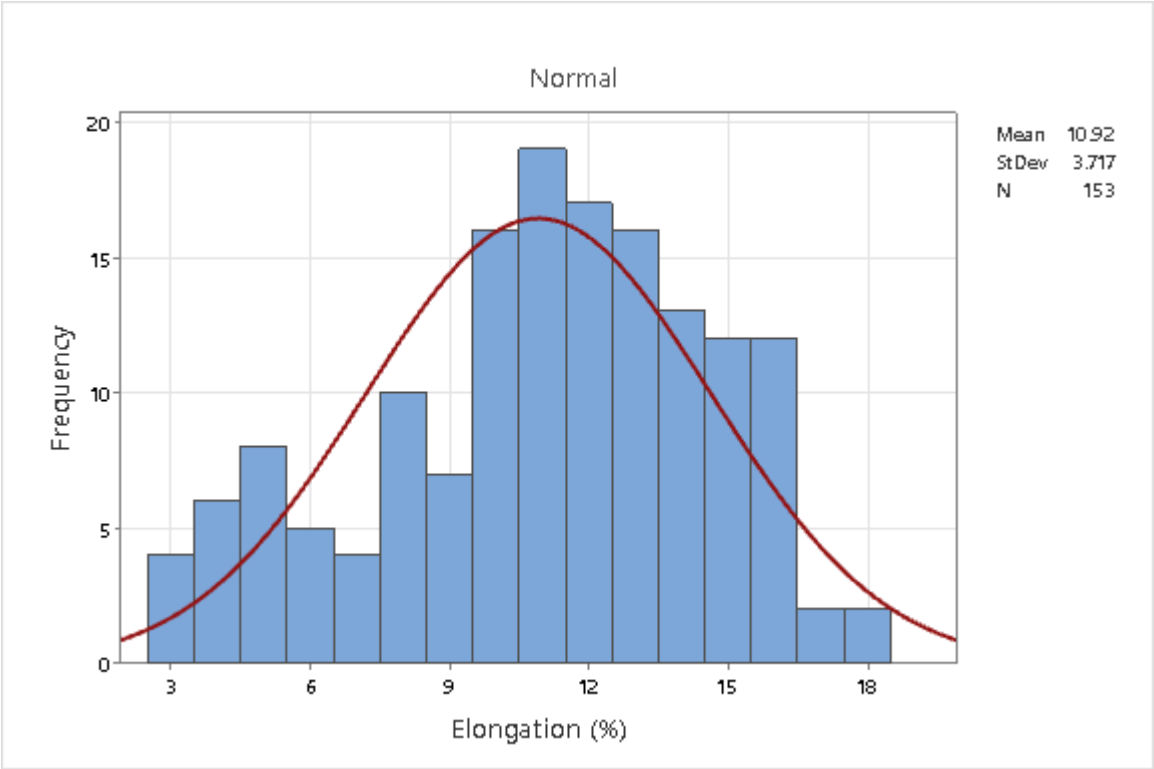

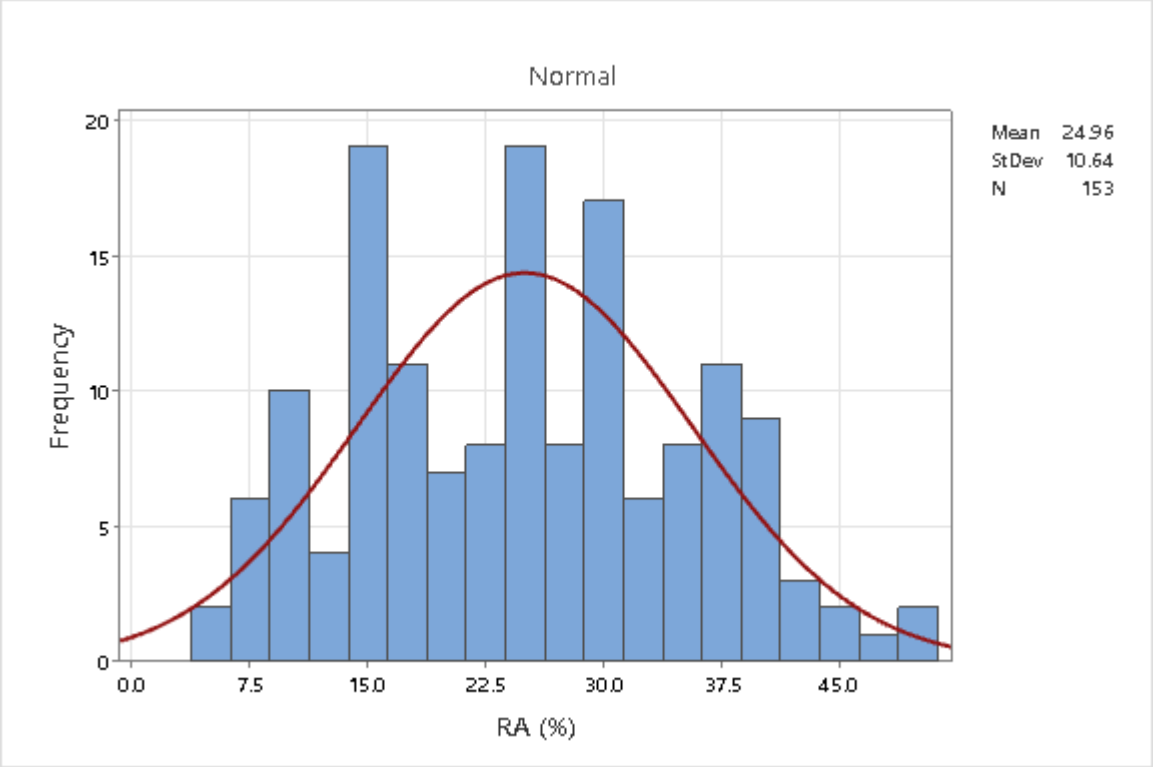

Figure 13 Histograms for ductility data with foundry “X” data removed. Elongation data is shown in (a) and reduction of area data is shown in (b).

The mechanical test data by the specimen ID locations is examined next. In Table 7 the tensile property test data statistics by specimen IDs for all foundries is given showing; the number of samples, mean, standard error of the mean, standard deviation, and minimum and maximum values. Table 8 provides the same statistics for the mechanical testing data except that the foundry X data are removed. Histograms of the strength and ductility data in Table 8 are plotted in Figures 14, 15, 16 and 17. In Figure 14 the location of the specimen ID is called out for specimen F1, and also the location of the scale for the plots is either at the top (as indicated in Figure 14) or at the bottom of the column of histograms. The same scale is used for a given property for all specimen IDs. In particular, looking at plots that are above or below one another, the shifting of the data left (lower values) or right (higher values) by specimen ID is readily apparent. Consider the *UTS* histograms of data for specimens H1 and V5 in Figure 14, there is a noticeable shift in the data to the right (higher strength) for the H1 compared to V5. Similarly, the *UTS* histograms for specimens H2 and V2 are shifted to higher strengths compared to V6. In Figures 14, 15, 16 and 17 the calculated normal probability distribution is shown by the maroon colored curves. The variability in the data by specimen location is reflected by the width of these curves. For example, the widths of the elongation distributions for specimens F1 and F2 in Figure 16 are remarkably different. The strength and ductility property data clearly depend on their location in the casting, both in terms of level and variability.

The dependency of the property measurements on location in the castings (or specimen ID) can be visualized using box plots using the elements discussed earlier with respect to Figure 10(a). Box plots of the strength data are given in Figure 18, and the ductility data box plots are shown in Figure 19. The highest strengths on average are observed in specimen IDs F2, H1, H2 and H3, and the variability in strength at those locations is relatively low. Conversely, the lowest strengths are observed in specimen IDs F1, V5 and V6, and the variability in strength at those locations is relatively high. This provides another demonstration that both the level and variability in strength properties vary by location in the castings. This trend is observed in the ductility data as well in the case of the elongation data in Figure 19(a). Here the ductility for specimens F2, H4 and V4 is higher with lower variability relative to the specimens with lower ductility, namely F1, V1, V3, V5 and V6. As a measure of ductility, the reduction of area *RA* has been regarded as a more problematic measurement compared to the elongation. This seems borne out as the variability in the *RA* measurements is noticeably higher than the elongation measurements in Figure 19. The difference in the variability between the *RA* and elongation measurements for specimen F2 is particularly striking. Specimen F2 also had the smallest diameter specimen size used in this investigation, and might be contributing to the variability in *RA* measurements. The next section explores whether results from casting and heat treatment processing simulations correlate with the property measurements and explain these observations.

Table 7 Tensile property test data statistics by specimen IDs showing: number of samples, mean, standard error of the mean, standard deviation, and minimum and maximum values.

Property	Specimen ID	N	Mean	SE Mean	StDev	Minimum	Maximum
UTS (ksi)	F1	16	118.85	2.65	10.59	99.20	141.20
	F2	16	135.91	2.90	11.60	114.20	150.00
	H1	16	133.99	2.51	10.02	114.10	143.30
	H2	15	134.11	2.86	11.09	112.30	145.80
	H3	15	133.80	2.82	10.94	112.30	144.00
	H4	16	131.75	2.40	9.59	111.40	141.90
	V1	16	129.66	2.53	10.11	109.30	140.90
	V2	16	133.04	2.50	10.00	114.30	142.90
	V3	15	123.41	2.70	10.44	101.90	139.60
	V4	16	129.91	2.49	9.96	109.60	139.90
	V5	16	119.84	2.22	8.87	102.10	133.30
	V6	16	118.62	2.49	9.97	103.20	137.60
YTS (ksi)	F1	16	97.61	3.46	13.85	73.20	127.30
	F2	16	121.29	3.58	14.33	94.20	139.20
	H1	16	119.30	3.09	12.36	94.50	130.40
	H2	15	119.22	3.56	13.78	92.10	133.80
	H3	15	118.76	3.45	13.35	92.60	131.70
	H4	16	116.32	3.18	12.71	90.70	128.30
	V1	16	114.51	2.93	11.71	92.50	128.60
	V2	16	117.25	3.04	12.16	94.10	129.00
	V3	15	104.67	3.58	13.87	78.30	126.90
	V4	16	112.66	3.07	12.29	89.30	127.50
	V5	16	102.05	3.15	12.61	79.80	124.80
	V6	16	99.39	2.99	11.98	81.70	127.20
Elongation (%)	F1	16	12.26	1.49	5.94	3.60	24.00
	F2	16	14.938	0.766	3.065	11.000	21.000
	H1	16	12.563	0.973	3.894	5.500	19.000
	H2	15	12.700	0.862	3.337	8.000	19.000
	H3	15	12.500	0.803	3.111	8.500	19.000
	H4	16	14.469	0.915	3.658	9.500	21.000
	V1	16	9.96	1.16	4.63	3.00	16.00
	V2	16	14.31	1.22	4.86	5.00	22.00
	V3	15	10.57	1.27	4.92	2.50	20.00
	V4	16	16.438	0.953	3.812	13.000	24.000
	V5	16	8.31	1.12	4.48	3.00	18.00
	V6	16	8.863	0.852	3.406	4.000	14.000
RA (%)	F1	16	26.16	3.14	12.57	9.50	53.00
	F2	16	37.56	2.26	9.03	18.00	51.00
	H1	16	28.31	2.38	9.52	14.00	45.00
	H2	15	26.40	2.25	8.73	16.00	45.00
	H3	15	27.33	2.11	8.16	16.00	45.00
	H4	16	36.38	2.13	8.51	25.00	52.00
	V1	16	22.13	2.84	11.35	7.00	40.00
	V2	16	33.97	3.88	15.52	6.00	55.00
	V3	15	21.70	2.94	11.38	7.50	50.00
	V4	16	41.50	2.36	9.44	28.00	59.00
	V5	16	15.34	1.73	6.94	7.50	29.00
	V6	16	18.03	1.74	6.95	5.50	32.00

Table 8 Tensile property test data statistics by specimen IDs **with Foundry "X" removed** showing: number of samples, mean, standard error of the mean, standard deviation, and minimum and maximum values.

Variable	Specimen ID	N	Mean	SE Mean	StDev	Minimum	Maximum
UTS (ksi)	F1	13	122.65	2.02	7.27	113.20	141.20
	F2	13	140.81	1.51	5.44	130.50	150.00
	H1	13	138.49	0.813	2.93	134.50	143.30
	H2	12	139.28	0.939	3.25	135.60	145.80
	H3	12	138.97	0.738	2.56	136.10	144.00
	H4	13	135.95	0.952	3.43	129.00	141.90
	V1	13	133.91	1.33	4.78	123.40	140.90
	V2	13	137.14	1.46	5.27	126.00	142.90
	V3	12	127.92	1.47	5.10	123.70	139.60
	V4	13	134.30	0.980	3.53	128.00	139.90
	V5	13	123.47	1.29	4.63	115.20	133.30
	V6	13	122.05	2.08	7.49	111.80	137.60
YTS (ksi)	F1	13	102.09	2.96	10.69	85.40	127.30
	F2	13	127.34	1.86	6.70	114.60	139.20
	H1	13	124.87	0.952	3.43	119.00	130.40
	H2	12	125.61	1.24	4.31	121.10	133.80
	H3	12	125.01	1.07	3.71	121.00	131.70
	H4	13	121.56	1.79	6.46	107.50	128.30
	V1	13	119.25	1.76	6.36	108.00	128.60
	V2	13	122.14	1.88	6.78	109.70	129.00
	V3	12	110.18	2.52	8.73	99.50	126.90
	V4	13	117.70	1.79	6.45	108.20	127.50
	V5	13	106.78	2.30	8.31	95.40	124.80
	V6	13	102.97	2.83	10.21	91.10	127.20
Elongation (%)	F1	13	10.08	1.08	3.90	3.60	16.00
	F2	13	13.769	0.533	1.922	11.000	16.000
	H1	13	11.077	0.691	2.490	5.500	15.000
	H2	12	11.292	0.509	1.764	8.000	14.000
	H3	12	11.208	0.498	1.725	8.500	14.000
	H4	13	13.115	0.675	2.434	9.500	16.000
	V1	13	8.88	1.23	4.43	3.00	15.40
	V2	13	12.69	1.05	3.79	5.00	17.00
	V3	12	8.542	0.820	2.840	2.500	12.000
	V4	13	14.846	0.517	1.864	13.000	18.000
	V5	13	6.923	0.957	3.451	3.000	13.000
	V6	13	8.446	0.978	3.528	4.000	14.000
RA (%)	F1	13	21.50	2.26	8.15	9.50	38.00
	F2	13	34.92	2.17	7.82	18.00	49.00
	H1	13	25.08	2.00	7.19	14.00	40.00
	H2	12	22.92	1.52	5.26	16.00	33.00
	H3	12	24.92	1.88	6.52	16.00	40.00
	H4	13	33.23	1.59	5.72	25.00	42.00
	V1	13	20.08	3.14	11.32	7.00	40.00
	V2	13	29.88	3.94	14.21	6.00	50.00
	V3	12	17.21	1.58	5.47	7.50	26.00
	V4	13	37.62	1.36	4.89	28.00	47.00
	V5	13	14.35	1.97	7.10	7.50	29.00
	V6	13	17.12	2.03	7.31	5.50	32.00

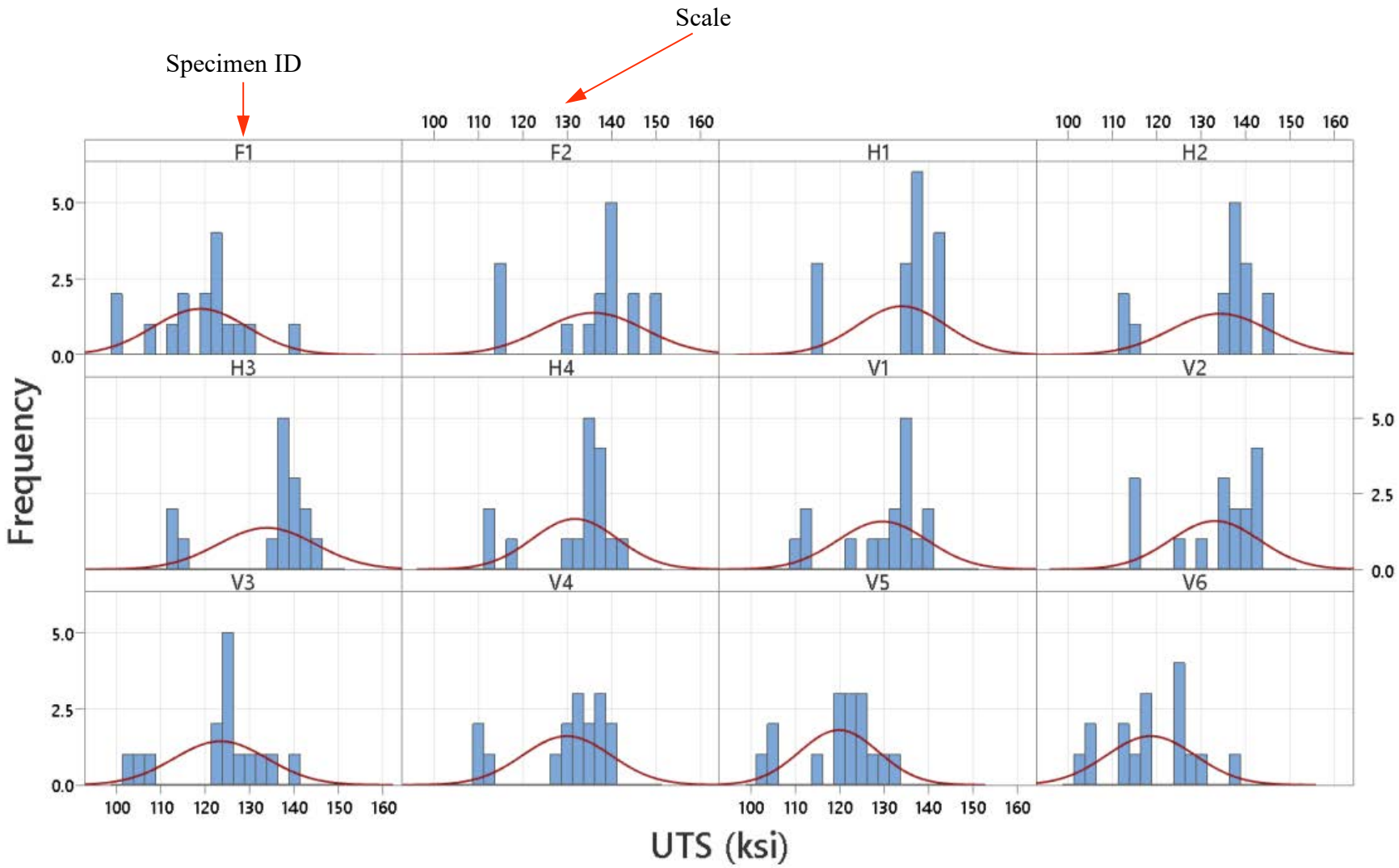

Figure 14 Histograms of the ultimate tensile strength data in Table 8 plotted by specimen ID (or location in the casting). Note that the specimen ID is labeled at the top/center above each plot, and that the same scale is used for each plot with its location alternating from the bottom to the top of the plots.

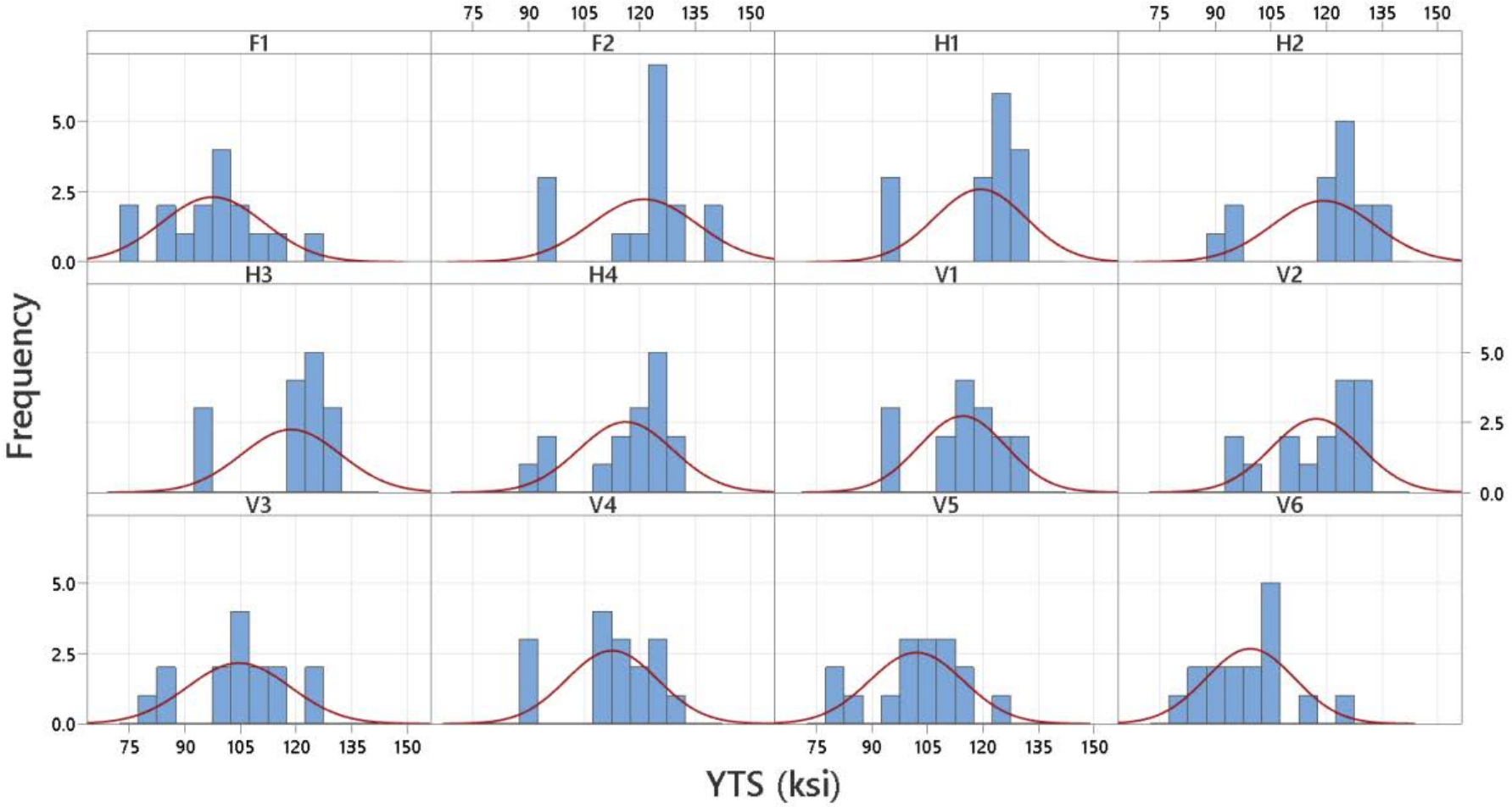

Figure 15 Histograms of the yield strength data in Table 8 plotted by specimen ID (or location in the casting).

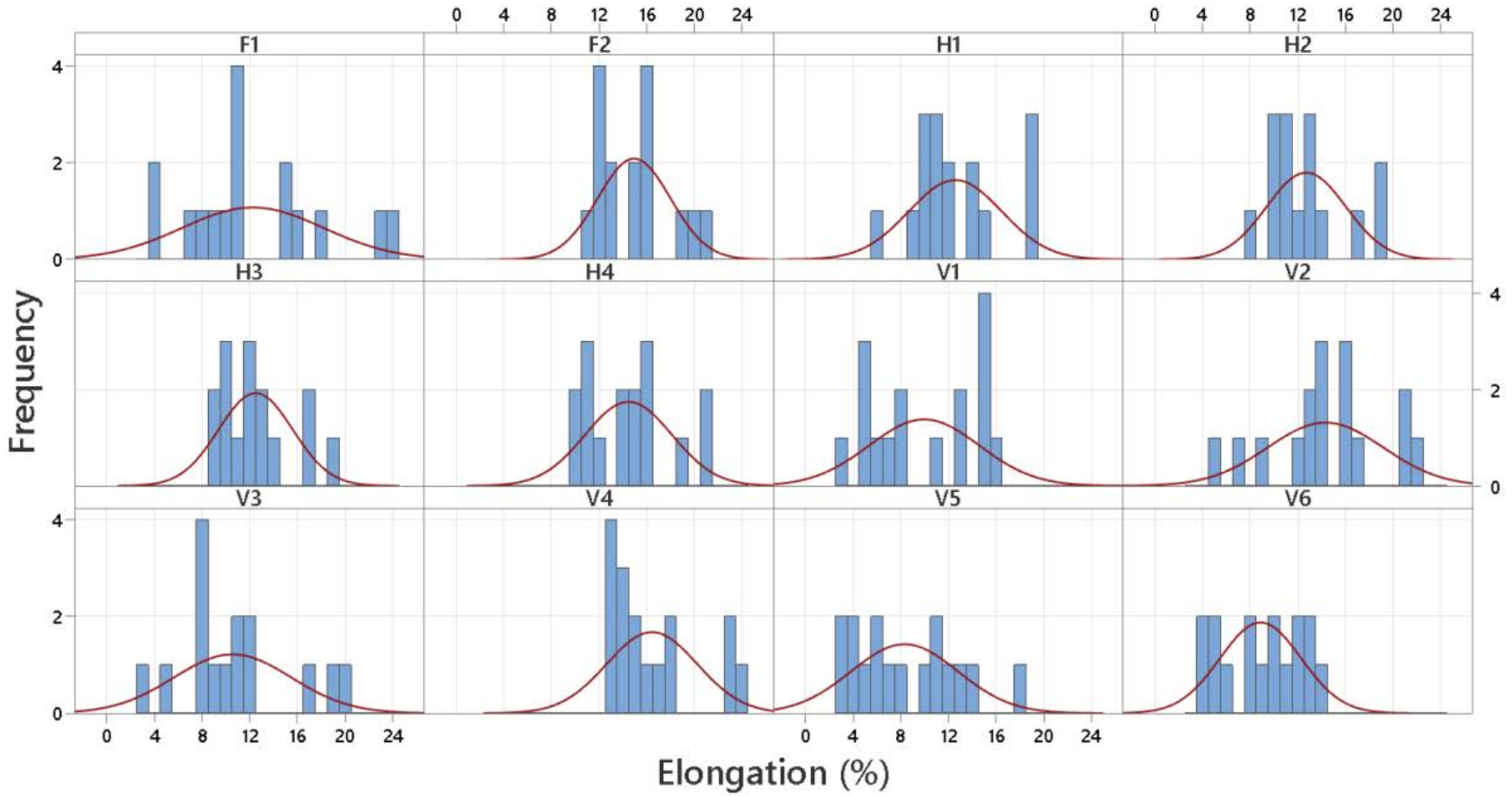

Figure 16 Histograms of the elongation data in Table 8 plotted by specimen ID (or location in the casting).

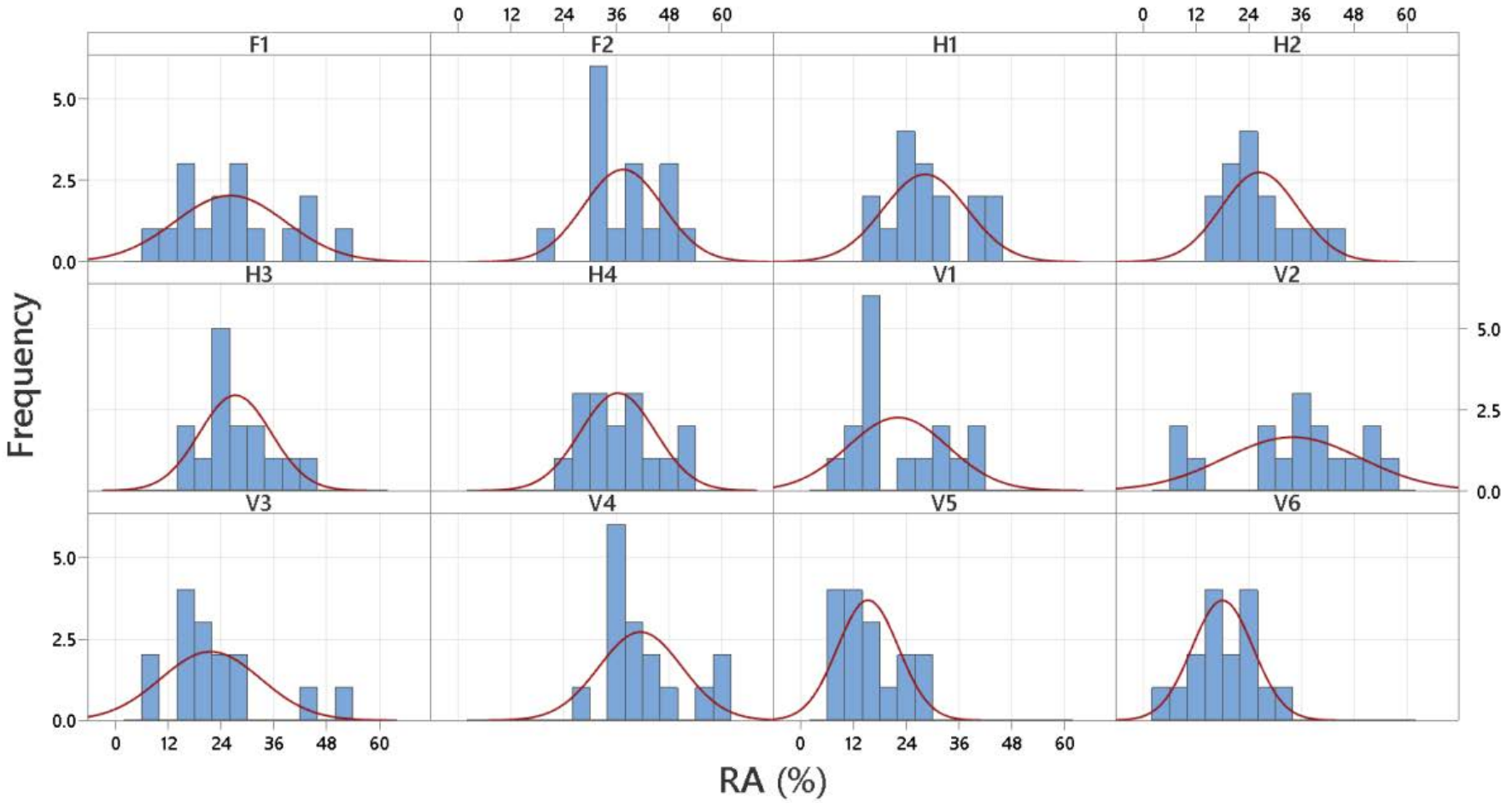

Figure 17 Histograms of the reduction of area data in Table 8 plotted by specimen ID (or location in the casting).

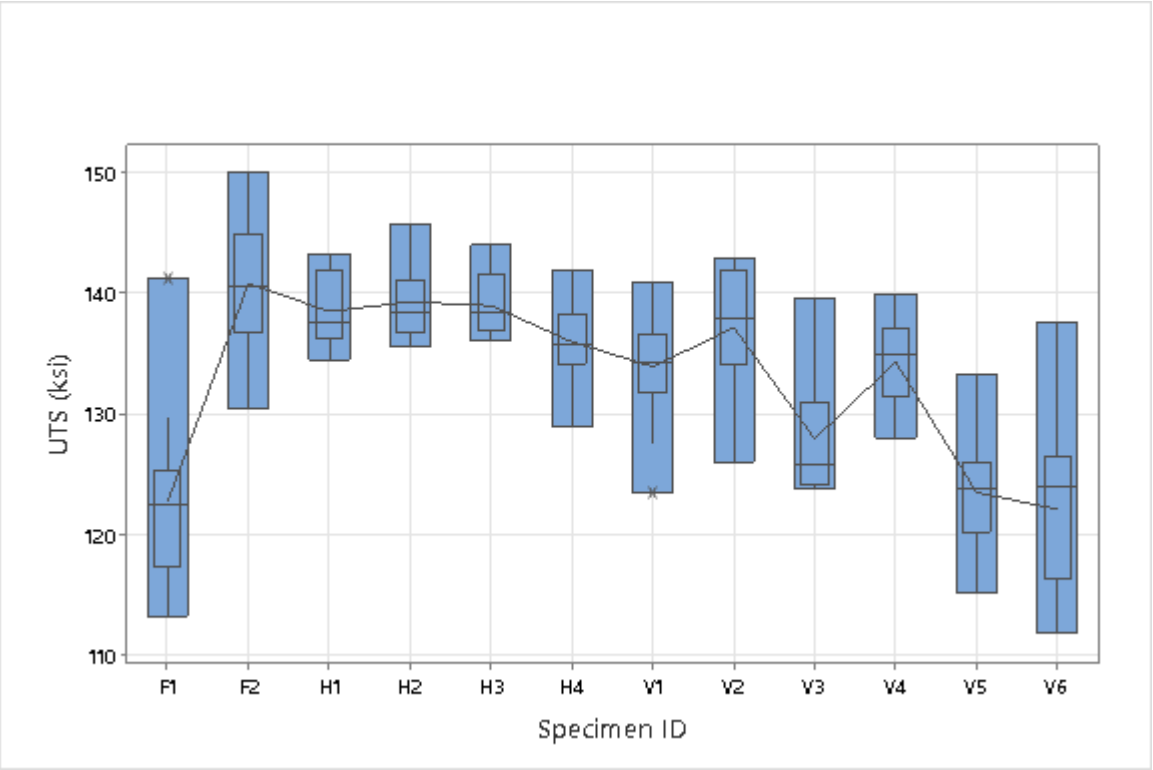

(a)

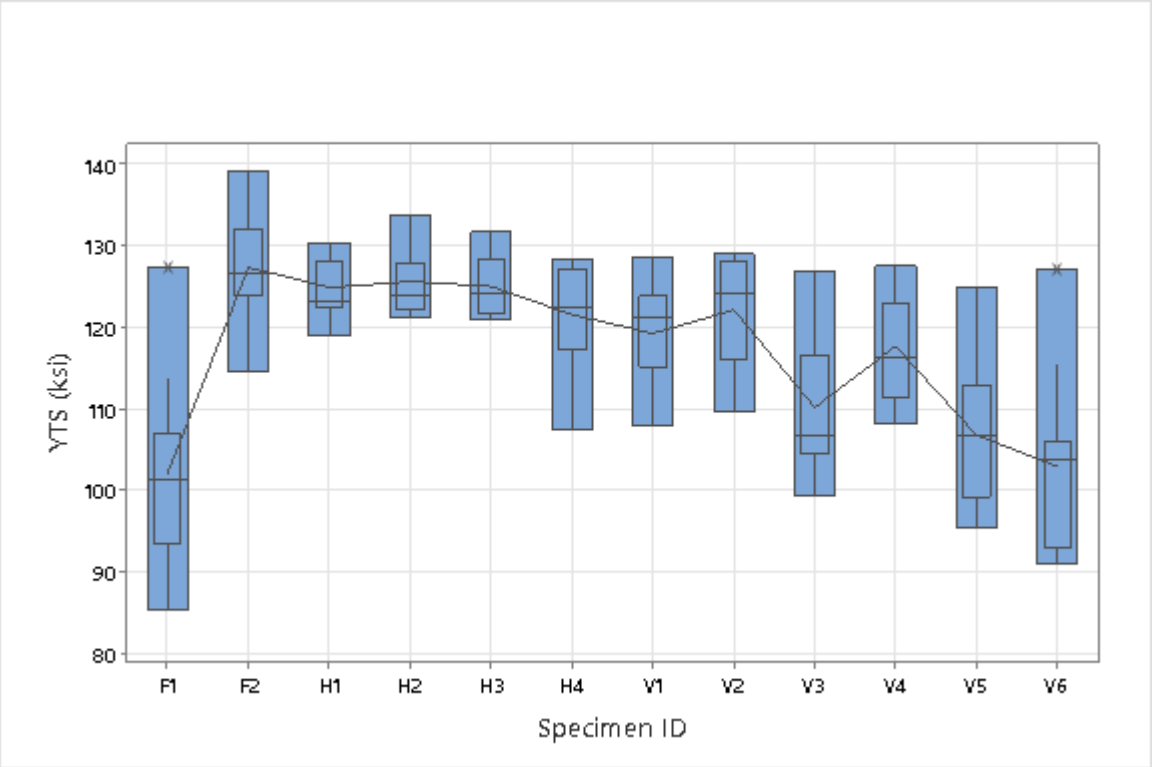

(b)

Figure 18 Box plots for strength data analyzed by specimen ID. *UTS* data is shown in (a) and yield strength data is shown in (b).

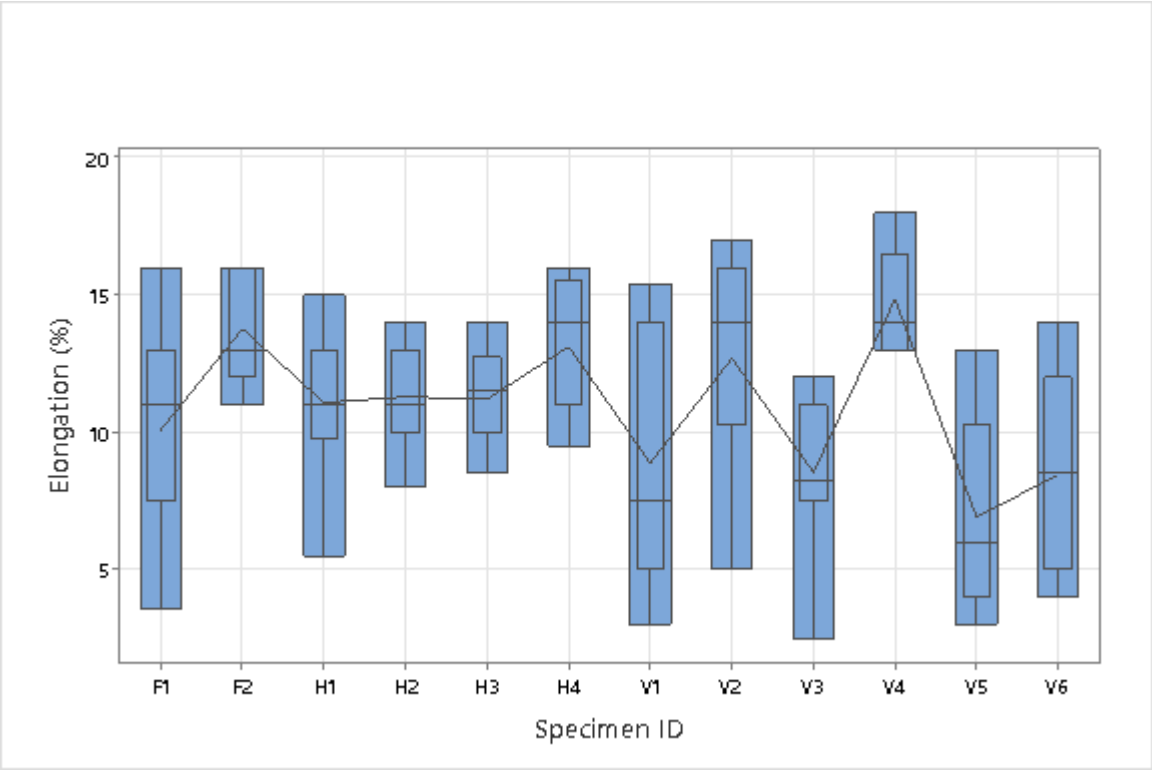

(a)

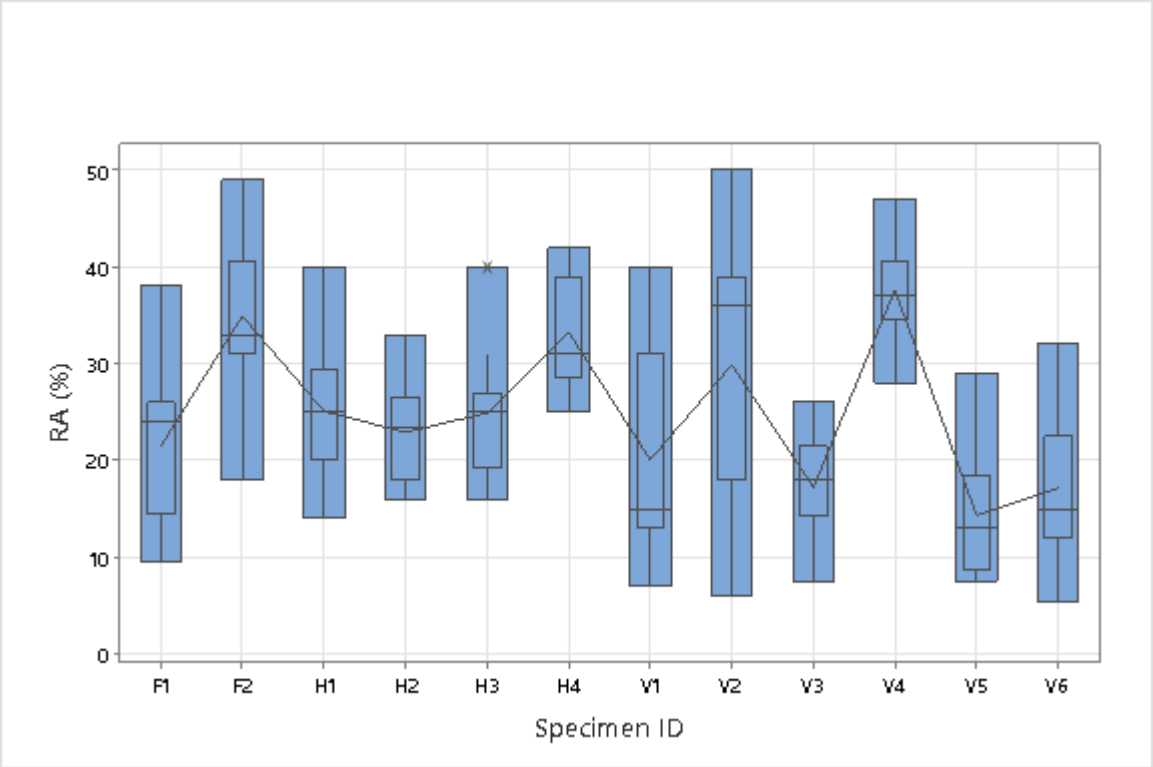

(b)

Figure 19 Box plots of ductility data analyzed by specimen ID. Elongation data is shown in (a) and reduction of area data is shown in (b).

5. Simulation Results and Properties

The analysis of the measurements and simulations is presented in this section. Relationships and correlations between results from solidification and heat treat simulations and measured tensile properties are reported below. Strength estimation calculations determined from previous work using casting and heat treatment simulation results are compared with the data measured in the current study. In the previous work, the strength estimations were determined based on a much smaller set of 18 tensile samples.

The six simulation results listed earlier are compared to tensile measurements. The first step applied to analyze the data is to generate a correlation table between the measured tensile data and the *MAGMAsoft* simulation results. The table gives the correlation coefficient *C* and p-value *p* for each combination of variables. As seen in Table 9, for each measured property in a given row (*UTS, YS, EL* and *RA*) the simulation results are arranged in columns from left to right in order of statistical significance. In Table 9 the *C,* p-value and number of samples *N* are called out as 0.57, <.0001 and 189, respectively, for the *UTS-T85* property-result variable combination. The correlation coefficients give the strength and direction of the relationship between the two variables. These range from -1 to +1, where -1 is a perfect negative correlation, +1 is a perfect positive correlation, and 0 indicates no correlation. The p-value is the probability of observing this relationship if the variables are correlated due to random chance. Low values indicate there is a low probability that the relationship is due to random chance; where below $p = 0.05$ the relationship is somewhat significant, and below $p = 0.0001$ the relationship is highly significant. The correlation table for all data in this study is given in Table 9 and the correlation table for the data with the foundry X data removed is given in Table 10. The relationships on the left hand side of the table in the red boxes are found to be highly statistically significant. Focusing on Table 10, with the foundry X data removed from the analysis, the simulation results; *T85*, solidification rate and cooling rate, are all found to have a highly statistically significant relationship to strength. Porosity is found to be fairly significant variable on the *UTS* ($p = 0.0026$), and somewhat significant on *YS* ($p = 0.048$). For the ductility data, highly significant simulations results on elongation are; the Niyama Criterion, its cooling rate, porosity, solidification rate and *T85* in decreasing order of significance. Not surprisingly, the same simulation results are highly significant for reduction of area; only the porosity and solidification rate swap places in the order of significance.

Plots of measured mechanical properties versus simulation results are given in Figures 20 through 29. The data from foundry X is not included in these plots. In the plots data for the specimens with the heat treatment performed on the specimen blanks after their removal from the casting are plotted using the blue square symbols to distinguish them from the specimen material removed from the heat treated casting (red triangle symbols). The horizontal bars in the plots give plus/minus one standard deviation of the simulation results; sampled as described earlier. As seen in Figure 20, the specimens from the heat treated blanks do not have the highest strengths. Overall in the figure, the strength data show a strong correlation with *T85* as observed in the correlation table. In Figure 21 there is a strong correlation for increasing strength with increasing solidification rate, and above around 0.2 °C/s the data shows fairly consistent *UTS* properties above 130 ksi. There is a similar trend for cooling rate in Figure 22, but its variation in the specimen is much larger. There is a trend for decreasing strength with increasing porosity in Figure 23, particularly for *UTS*.

Table 9 Correlation table for the tensile measurements versus the simulation results for all specimens in the study.

UTS (ksi)	T85	SolRT	CoolRT	Porosity	Niyama	Grad Ave
C	0.57022	0.45689	0.43736	-0.17528	0.11177	-0.07930
p	<.0001	<.0001	<.0001	0.0158	0.1257	0.2780
N	189	189	189	189	189	189
YTS (ksi)	T85	SolRT	CoolRT	Porosity	Grad Ave	Niyama
	0.58795	0.46452	0.43486	-0.13234	-0.09107	0.07320
	<.0001	<.0001	<.0001	0.0695	0.2127	0.3169
	189	189	189	189	189	189
Elongation (%)	Niyama	Porosity	CoolRT	SolRT	T85	Grad Ave
	0.41041	-0.35042	0.34434	0.32572	0.25235	0.11374
	<.0001	<.0001	<.0001	<.0001	0.0005	0.1192
	189	189	189	189	189	189
RA (%)	Niyama	CoolRT	Porosity	SolRT	T85	Grad Ave
	0.49302	0.42707	-0.42579	0.39368	0.26519	0.15404
	<.0001	<.0001	<.0001	<.0001	0.0002	0.0343
	189	189	189	189	189	189

Table 10 Correlation table for the tensile measurements versus the simulation results for specimens in the study with the foundry X data removed.

UTS (ksi)	T85	SolRT	CoolRT	Porosity	Niyama	Grad Ave
	0.77697	0.70337	0.63603	-0.24171	0.15747	-0.11346
	<.0001	<.0001	<.0001	0.0026	0.0519	0.1626
	153	153	153	153	153	153
YTS (ksi)	T85	SolRT	CoolRT	Porosity	Grad Ave	Niyama
	0.75897	0.67246	0.59391	-0.16031	-0.12894	0.09275
	<.0001	<.0001	<.0001	0.0478	0.1122	0.2542
	153	153	153	153	153	153
Elongation (%)	Niyama	CoolRT	Porosity	SolRT	T85	Grad Ave
	0.47756	0.45979	-0.44261	0.42462	0.37845	0.12292
	<.0001	<.0001	<.0001	<.0001	<.0001	0.1301
	153	153	153	153	153	153
RA (%)	Niyama	CoolRT	SolRT	Porosity	T85	Grad Ave
	0.51185	0.50258	0.45300	-0.44685	0.31574	0.14988
	<.0001	<.0001	<.0001	<.0001	<.0001	0.0644
	153	153	153	153	153	153

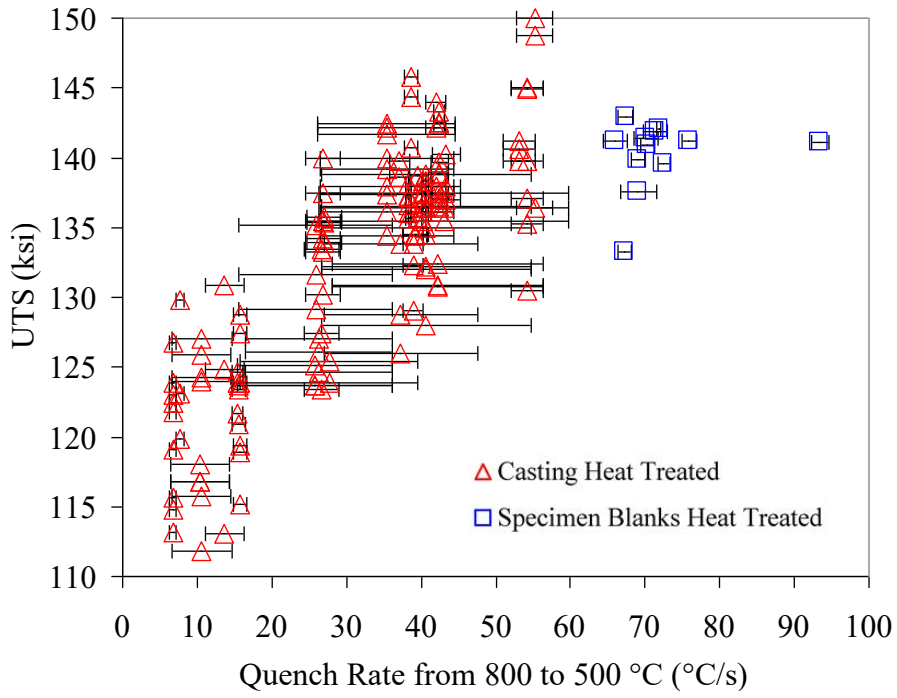

(a)

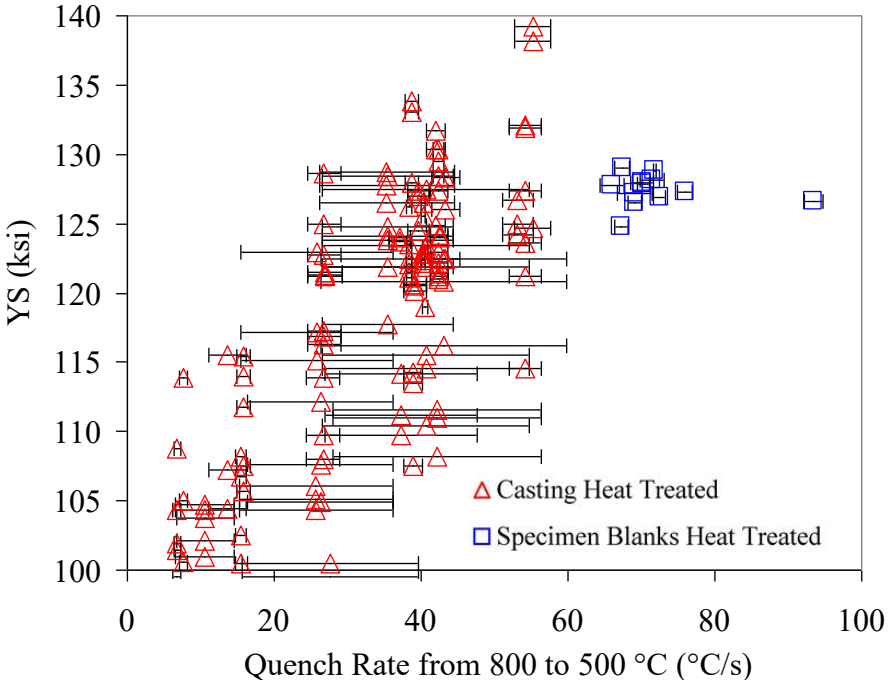

(b)

Figure 20 Measured strength data versus *T85* for specimens from heat treated castings and specimens from heat treated blanks. *UTS* data is shown in (a) and *YS* data is shown in (b).

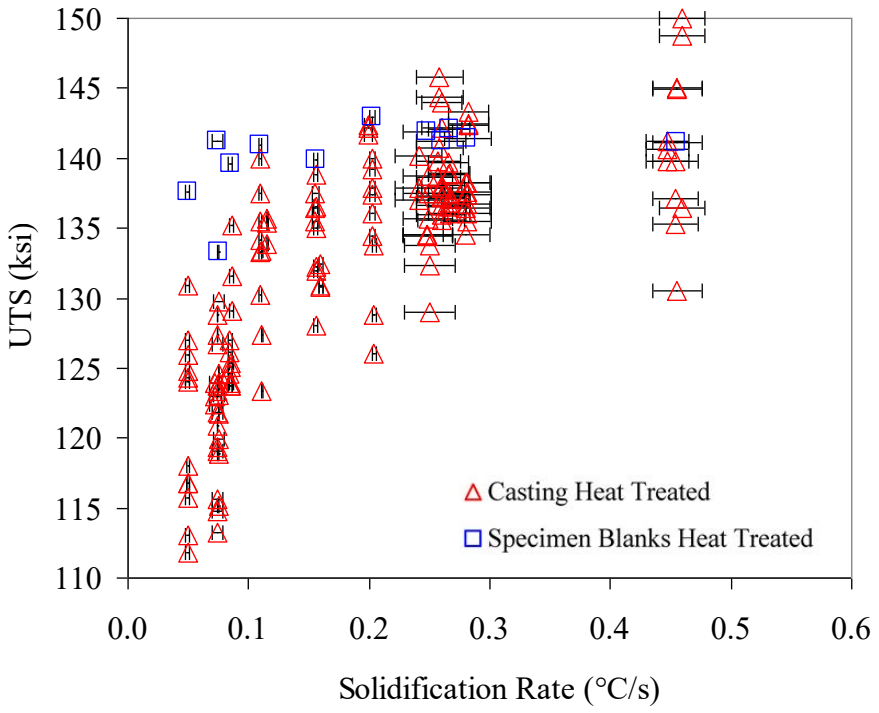

(a)

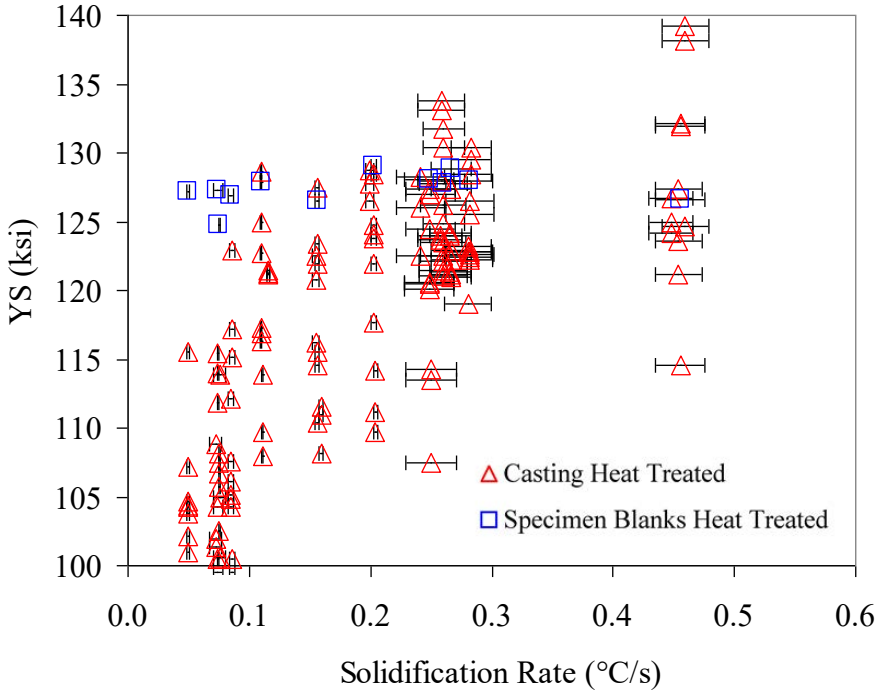

(b)

Figure 21 Measured strength data versus solidification rate for specimens from heat treated castings and specimens from heat treated blanks. *UTS* data is shown in (a) and *YS* data is shown in (b).

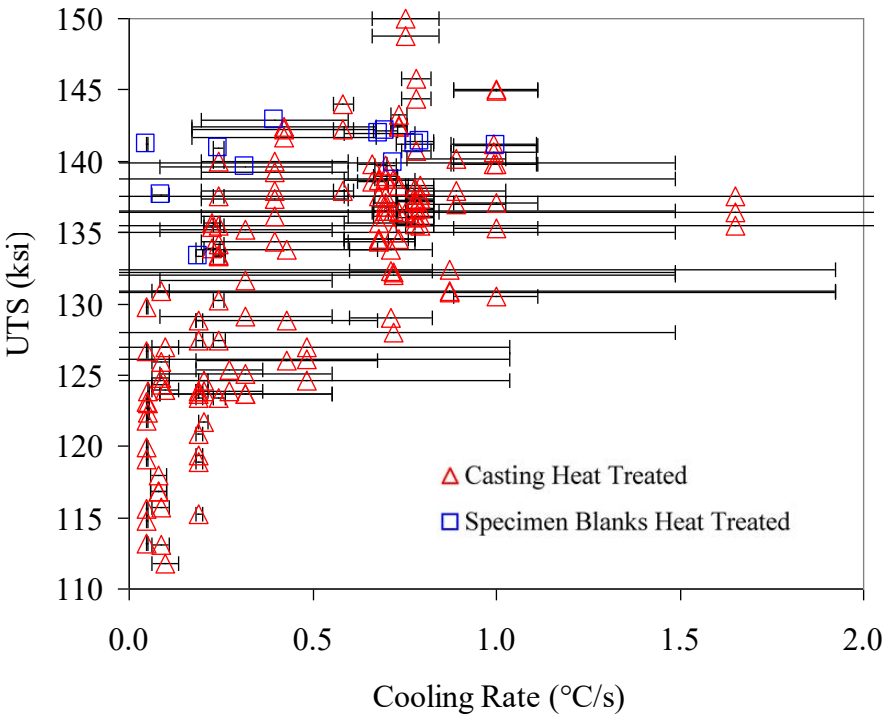

(a)

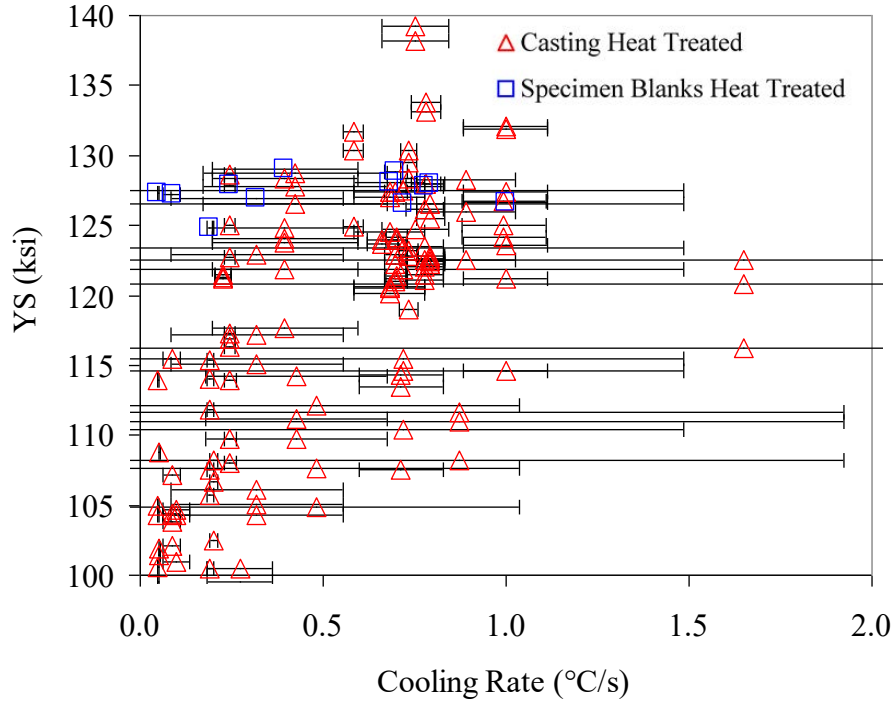

(b)

Figure 22 Measured strength data versus cooling rate for specimens from heat treated castings and specimens from heat treated blanks. *UTS* data is shown in (a) and *YS* data is shown in (b).

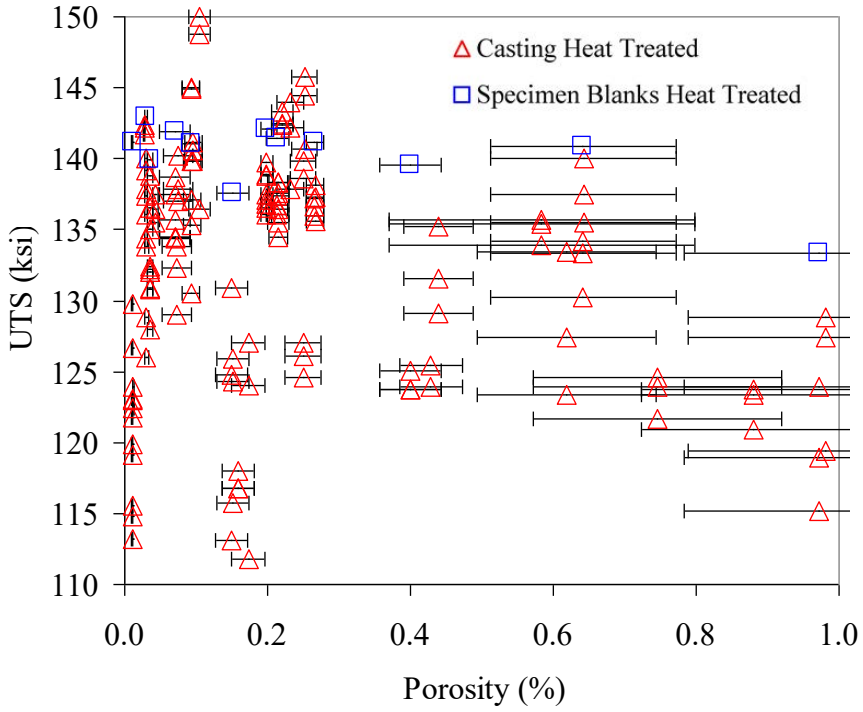

(a)

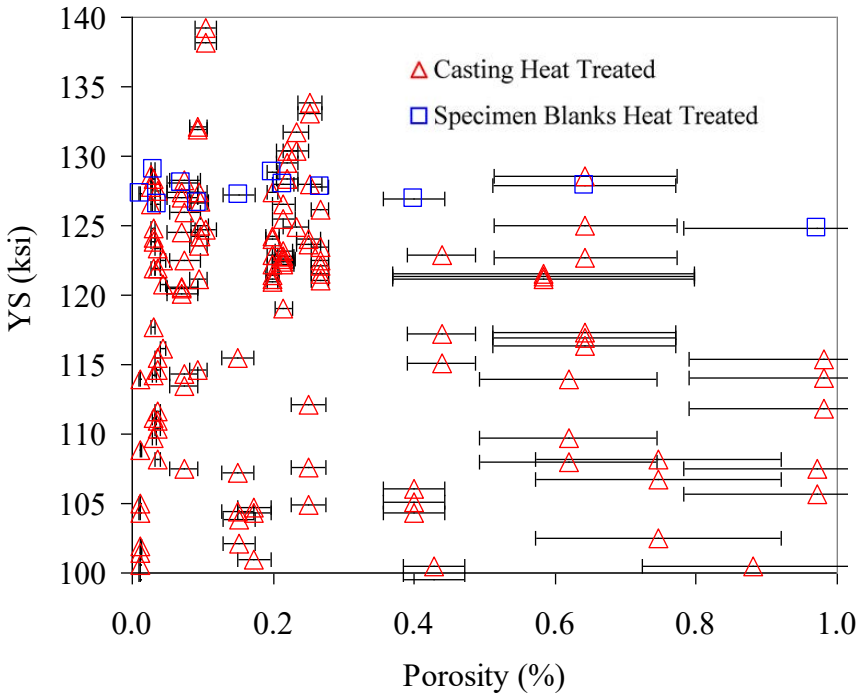

(b)

Figure 23 Measured strength data versus porosity prediction for specimens from heat treated castings and specimens from heat treated blanks. *UTS* data is shown in (a) and *YS* data is shown in (b).

Given that there are multiple variables affecting the mechanical strength properties, it is useful to look at the data for the specimens where the blanks were removed from the casting before being heat treated. These specimens all have essentially the same effect of the quench with uniformly high *T85* data as seen in Figure 20. The strength of these specimens is plotted versus porosity in Figure 24. There is about a 10 ksi reduction in *UTS,* and a 4 ksi reduction in *YS,* as the predicted porosity increases from a very low level to around 1%. Porosity in this predicted range seems to have a secondary role in the resulting strength, but might be considered in our future correlation work for predicting material properties if additional data becomes available.

In this study correlations between the measured ductility and the simulation results show a strong statistical significance with the porosity results (Niyama Criterion and porosity volume percentage), and the cooling and solidification rates. The plots for this data in Figures 25 to 29 appear more scattered than the strength results did. While more variables than porosity affect the ductility, it is well known that porosity (microporosity in particular for steel that can appear sound from NDE) reduces the ductility of a steel alloy and heat treatment like 8630 Q&T. This reduction in ductility can also be accompanied by a reduction in fatigue strength. The Niyama Criterion results in Figure 25, show that more data have higher ductility at higher result values. Since the more porosity is expected at lower Niyama Criterion values, this result is not surprising. However, there is a lot of scatter in Figure 25, and lower ductility at higher Niyama Criterion values in some cases, and vice versa. Similarly, in Figures 26 and 27 there are more consistently high ductility measurements at the highest cooling and solidification rates. At moderate rates though, there is considerably more scatter. In Figure 28 at higher porosity levels the specimens appear to have lower ductility, again though, not is every case. At low porosity levels, there is again evidence that more variables affect the ductility than just porosity. Specimens in the low porosity range have amongst both the highest, and the lowest, ductility, ranging from 4% to 18% elongation.

In an earlier study examining the lower bounds of strength data for cast 8630 Q&T steel [4], strength data for 18 specimens and simulation results were analyzed and a correlation between them was determined. Strength estimations were determined based on that relatively small data set of 18 tensile samples compared to over 150 tensile samples in this study for data from the commercial platypus castings. The ultimate strength estimation equation from the 18 test specimens was

$$UTS\,(\text{ksi}) \;=\; 108.3 + 0.453\,T85 + 19.8\,\dot{T} \tag{1}$$

where *T85* is the cooling rate between 800 °C and 500 °C during the quenching process, and $\dot{T}$ is the cooling rate used in Niyama Criterion. The yield strength estimation equation is determined from the *UTS* from Equation (1) using

$$YS\,(\text{ksi}) \;=\; 1.075\,UTS - 34.48 \tag{2}$$

Using the above equations, calculated versus measured strength data from the previous 8630 Q&T study are given in Figure 30. Lower bounds of 1% (red lines) and 10% (blue lines) are calculated for the data points and are given in the figure. The standard errors of the fits for Equations (1) and (2) are 6.0 and 3.5 ksi for the *UTS* and *YS*, respectively.

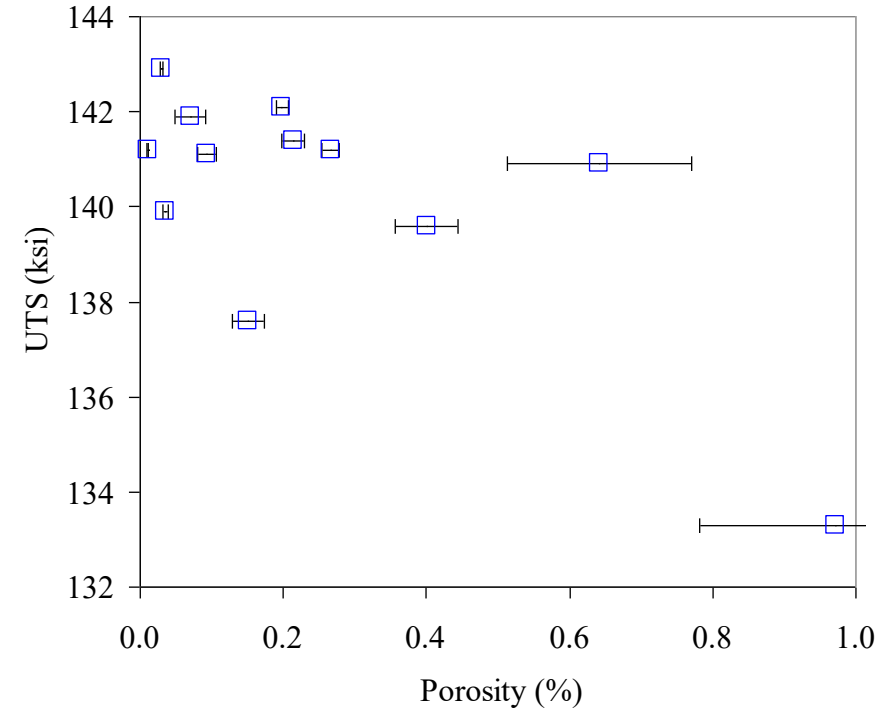

(a)

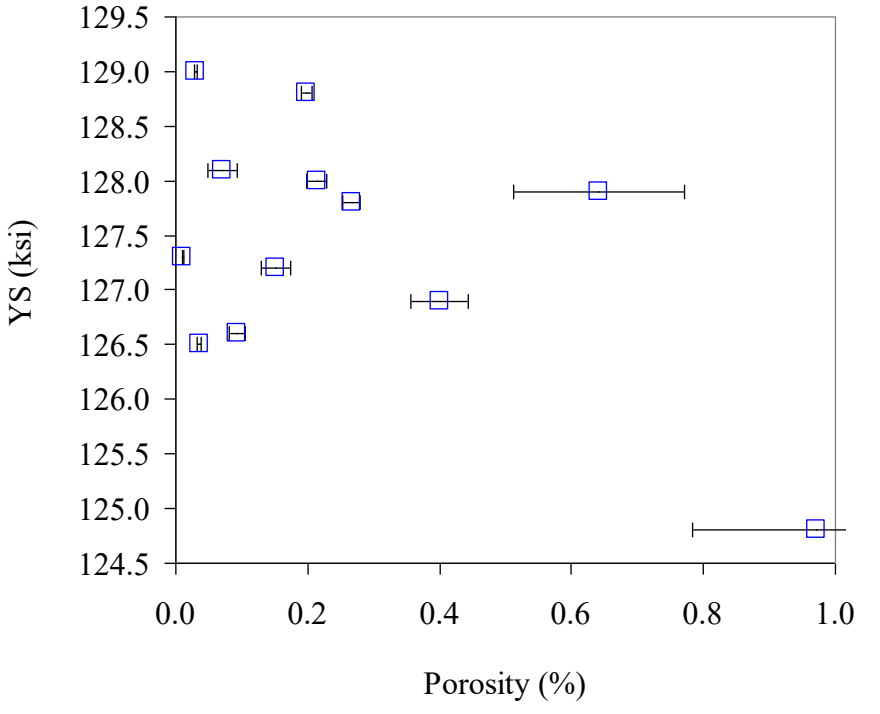

(b)

Figure 24 Measured strength data versus porosity prediction for the specimens with the heat treatment performed on the specimen blanks after their removal from the casting. *UTS* data is shown in (a) and *YS* data is shown in (b).

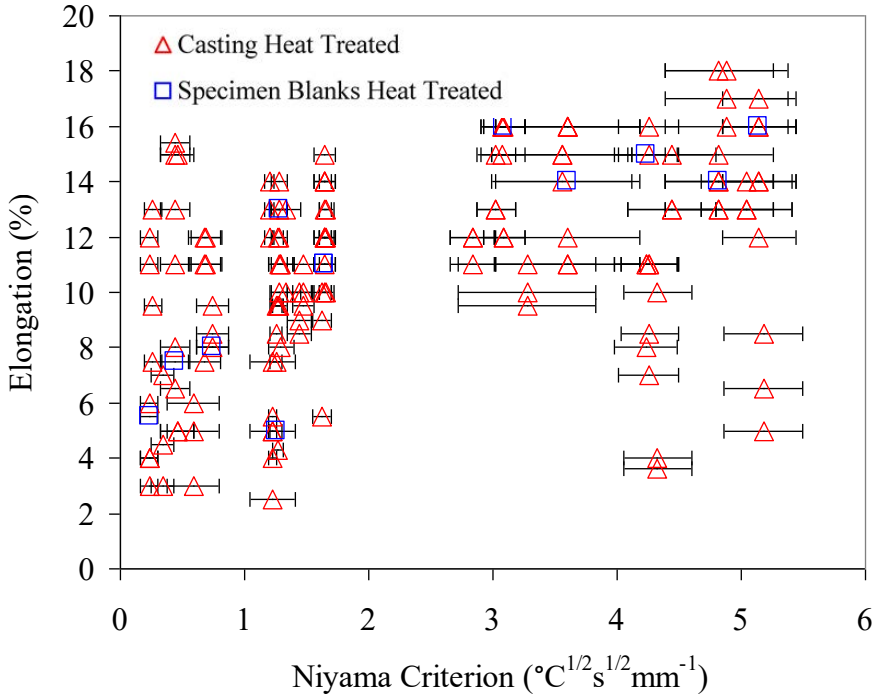

(a)

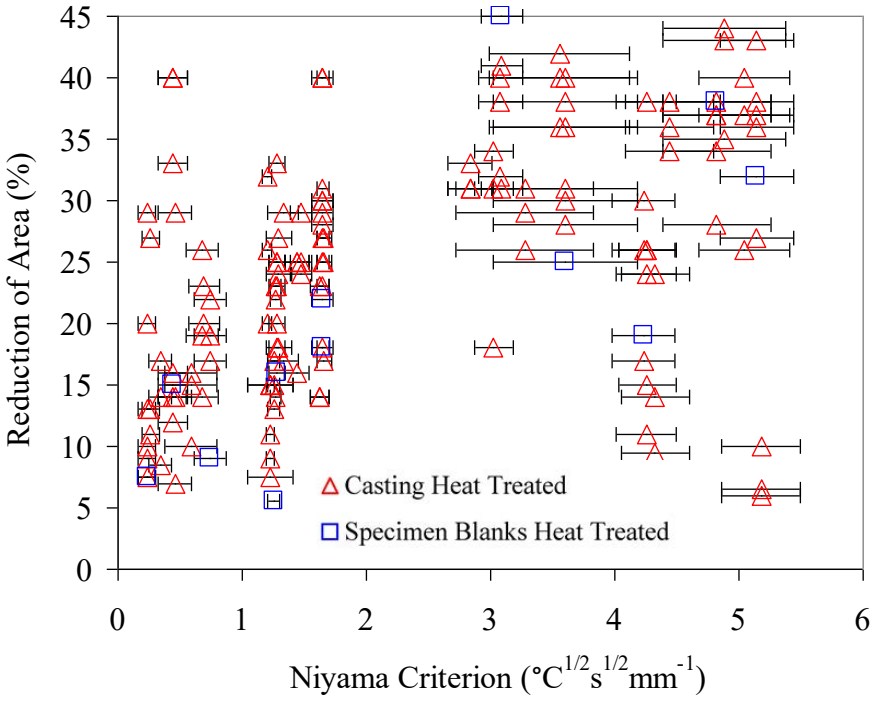

(b)

Figure 25 Ductility measurements versus Niyama Criterion prediction for specimens from heat treated castings and specimens from heat treated blanks. Elongation is shown in (a) and reduction of area shown in (b).

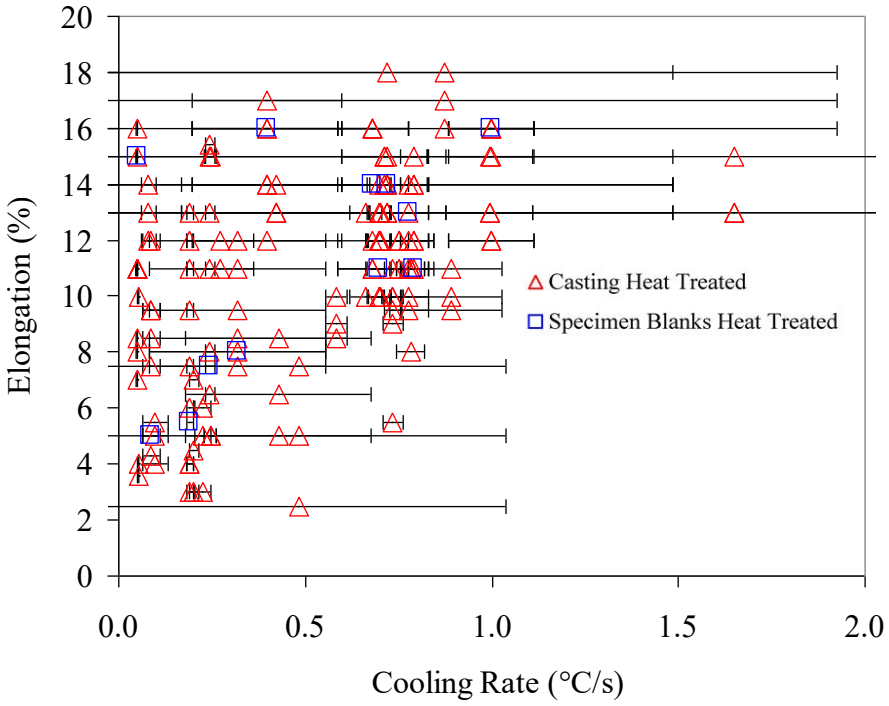

(a)

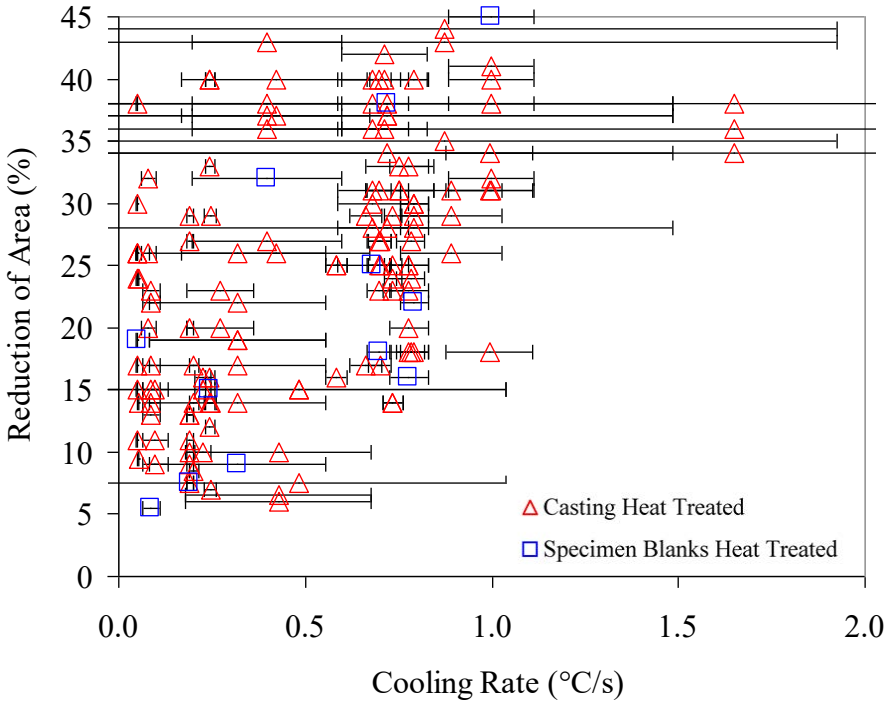

(b)

Figure 26 Ductility measurements versus cooling rate prediction for specimens from heat treated castings and specimens from heat treated blanks. Elongation is shown in (a) and reduction of area shown in (b).

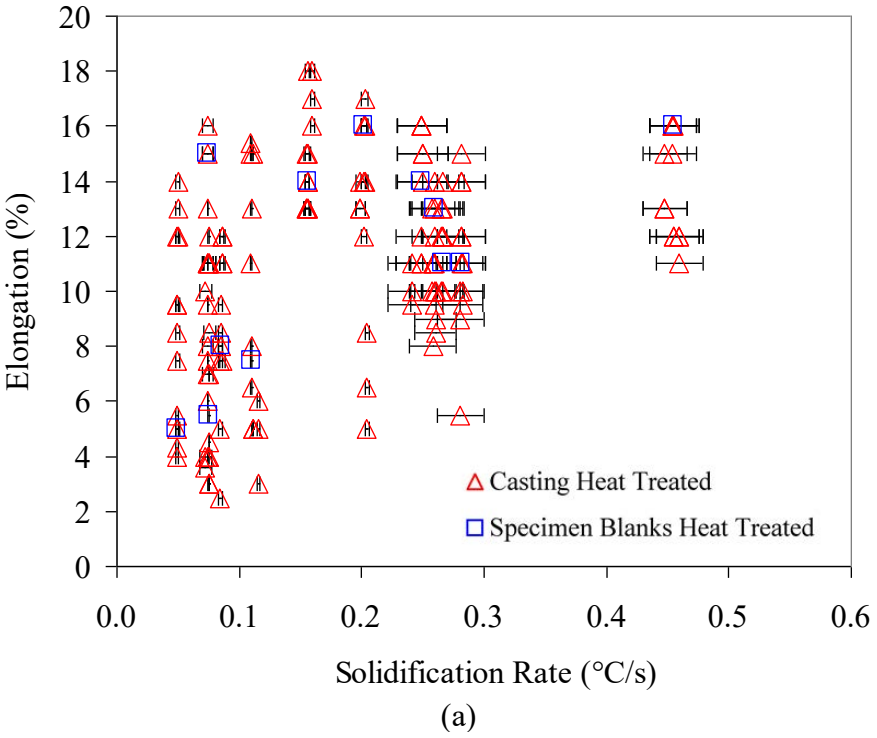

(a)

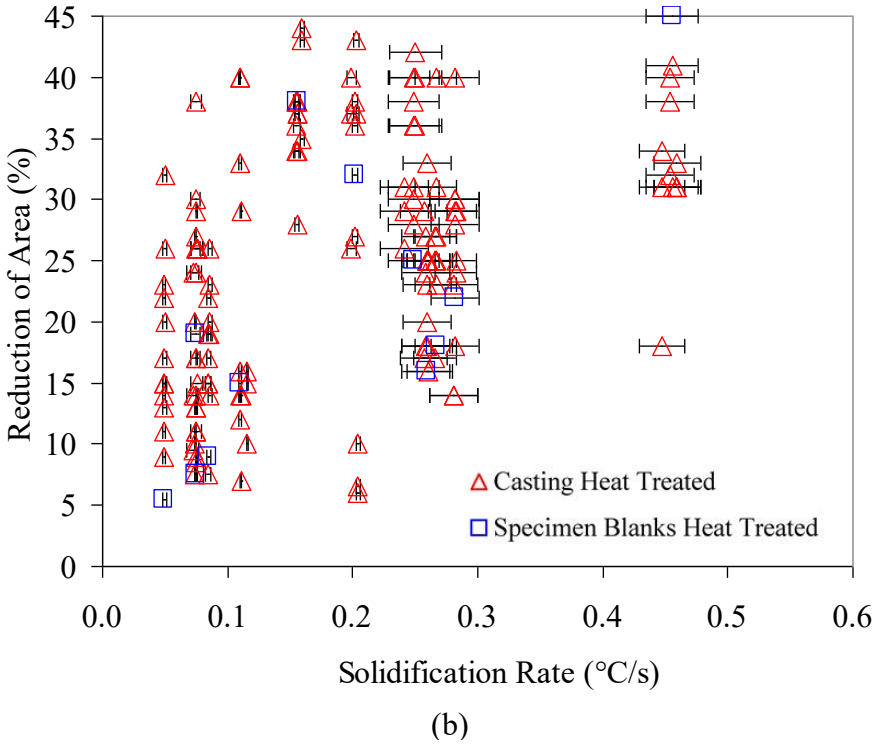

(b)

Figure 27 Ductility measurements versus solidification rate for specimens from heat treated castings and specimens from heat treated blanks. Elongation is shown in (a) and reduction of area shown in (b).

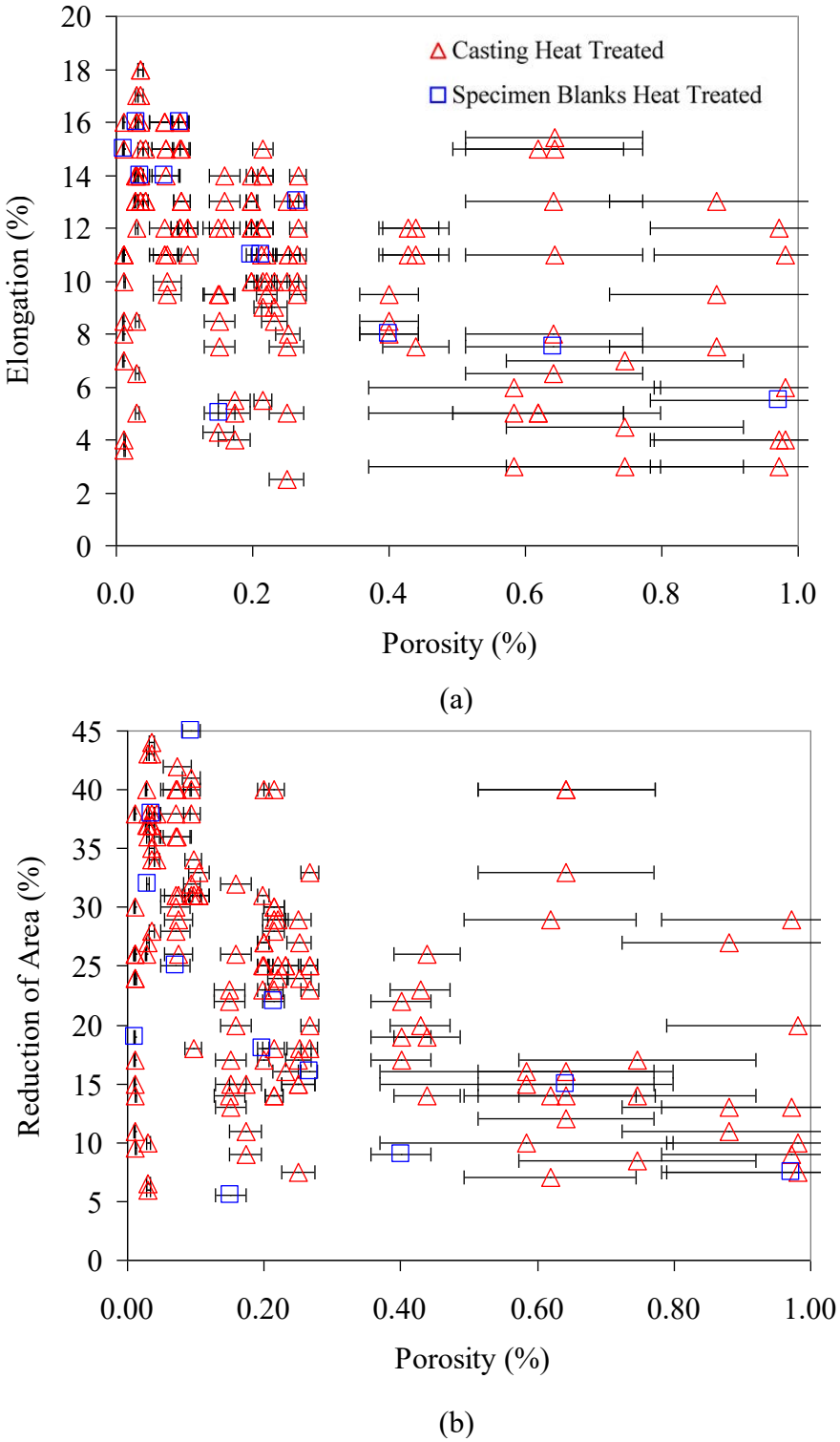

Figure 28 Ductility measurements versus porosity prediction for specimens from heat treated castings and specimens from heat treated blanks. Elongation is shown in (a) and reduction of area shown in (b).

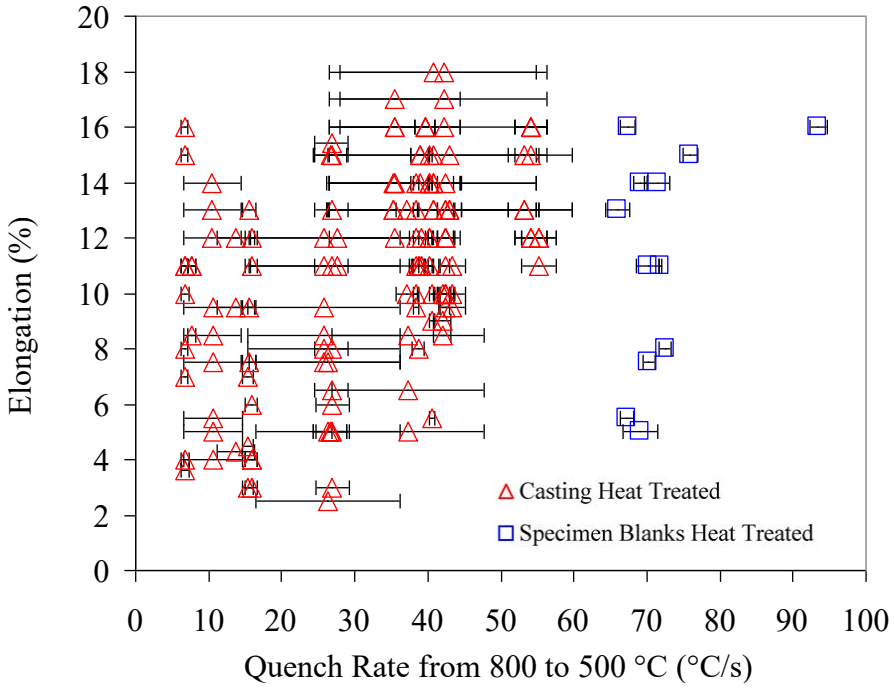

(a)

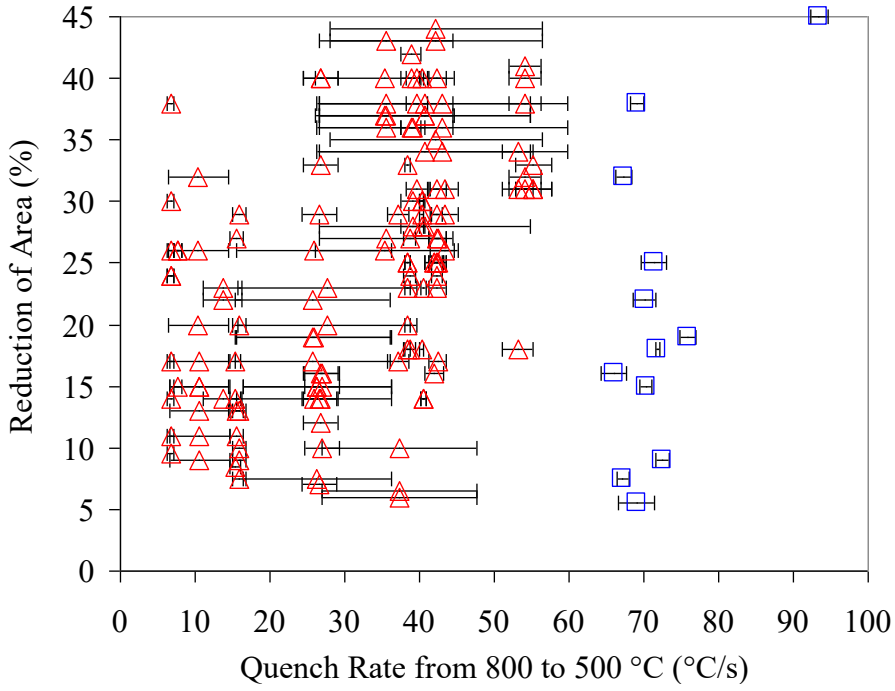

(b)

Figure 29 Ductility measurements versus quench cooling rate between 800 °C and 500 °C (*T85*) for specimens from heat treated castings and specimens from heat treated blanks. Elongation is shown in (a) and reduction of area shown in (b).

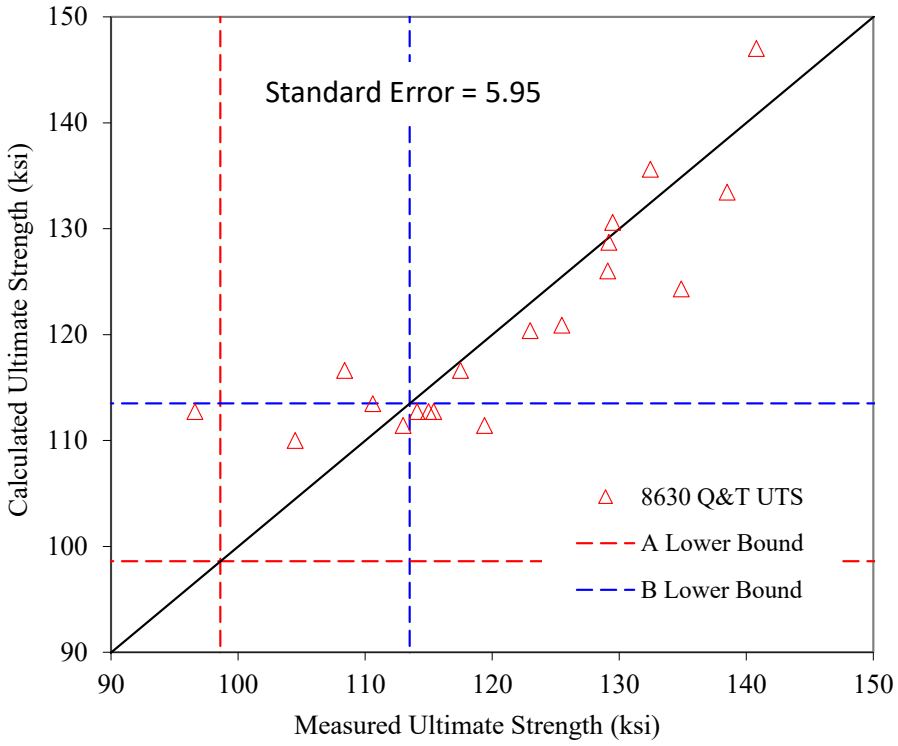

(a)

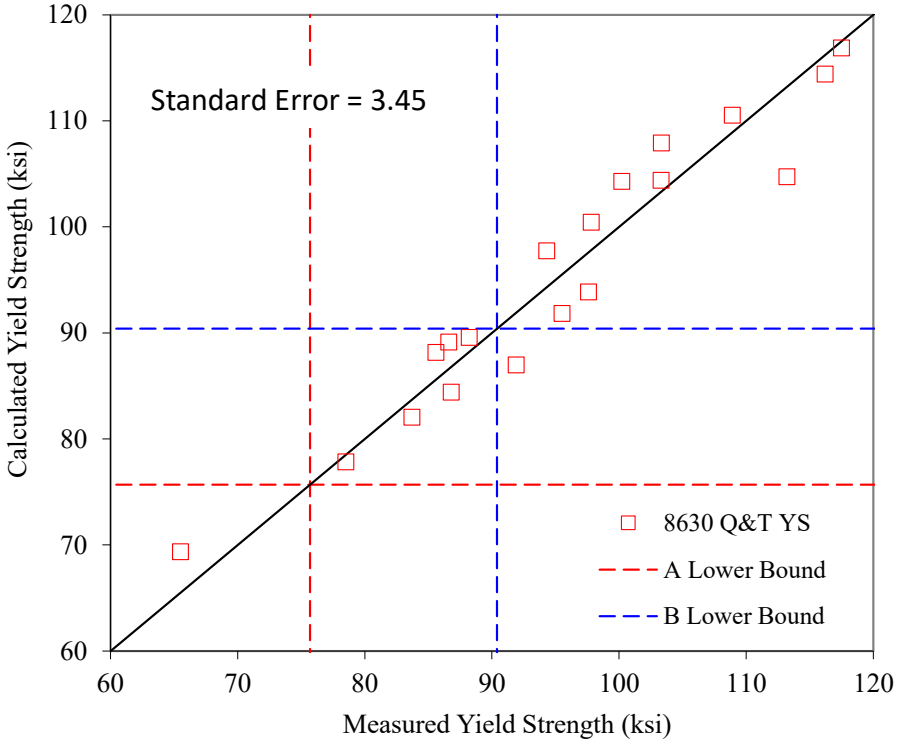

(b)

Figure 30 Calculated versus measured strength data using equations (1) and (2) fit to the plotted measured data from a study having a smaller sample size of 18 data points from 8630 Q&T castings. Lower bounds were calculated for the data points plotted here.

Using the fits from Equations (1) and (2), measured and calculated *UTS* and *YS* in are plotted in Figure 31 for the commercial casting platypus data. The calculated data from the present study compare well with the measurements, and the standard errors of the calculations are 8.7 and 12.0 ksi for the *UTS* and *YS*, respectively. The 1% and 10% lower bound properties plotted in Figure 31 as dashed red and blue lines, respectively. These are calculated from a large sample size of SFSA member data [5] of over 1560 data points.

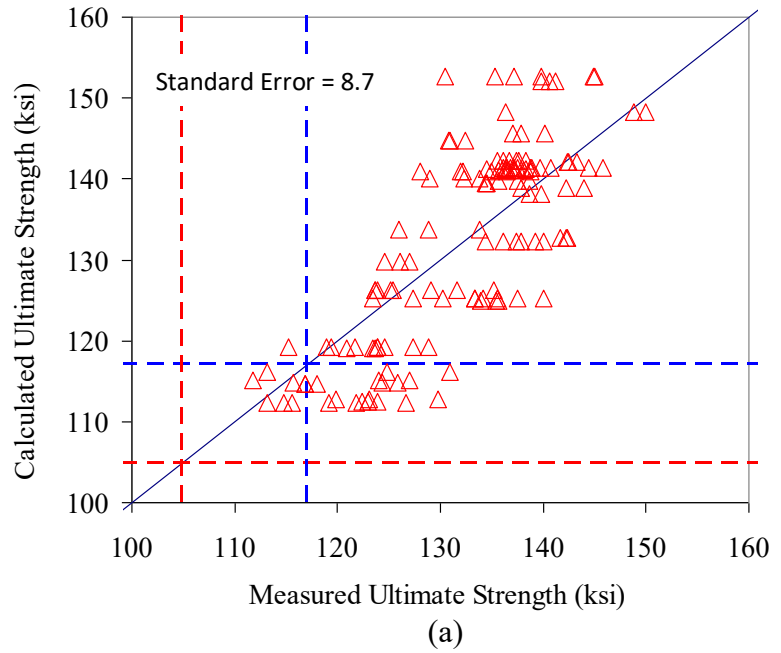

(a)

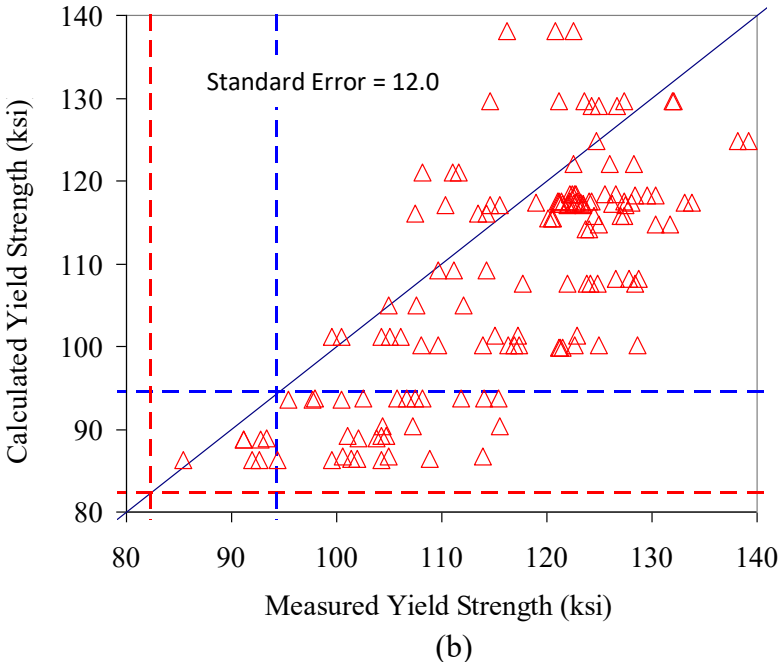

(b)

Figure 31 Calculated versus measured strength data using Equations (1) and (2) for the present study. Lower bound property data is from SFSA member data [5], approximately 1560 data points.

In the previous study involving the data plotted in Figure 30, most of the specimens were taken from test bars (Y-blocks, keel blocks and equivalent round bars). Only six of the specimens were taken from castings intended for commercial use. Only these are therefore comparable to the data set in the present study in terms of variability.

Judging from Figure 31, the previously determined correlations in Equations (1) and (2) appear to be applicable to the commercial castings in several respects. While the errors between strength measurements and estimates in Figure 31 are around twice those in Figure 30, the sample size in much larger, and there numerous other factors such as the casting to casting, foundry to foundry, and location variability in the data from the present study. Despite this, the previously determined estimations produce a good trend between measurements and estimations in Figure 31. Also, the calculated strengths are conservative in the lower range of strength measurements. In the upper range of measured strength, the data falls fairly equally on both sides of the line of agreement between measurement and calculation.

The applicability of the property estimates to commercial castings is also supported with respect to the lower bound strength properties. Neither measurements nor estimations are below the 1% lower bound (red dashes lines) in Figure 31 so they are conservative estimates. Just considering the measurements, these results support using these lower bound values for *UTS* and *YS* as conservative design properties for nominally sound commercial castings. By nominal meaning, some small amount of porosity that might affect ductility is tolerable. The maximum porosity predicted in the current study was 1.2% (plus one standard deviation above the mean in the gage section). In terms of the 10% lower bound strength data (blue dashed lines), it appears that seven measurement points fall below the 10% lower bound (about 4.6% of the data points), and a much larger number of estimated data points do as well. For the estimated data, this again indicates that Equations (1) and (2) are conservative for the data collected in this study. The use of these strength estimates will provide reasonably accurate and conservative estimates of the strength variations and inhomogeneities in 8630 Q&T steel castings.

6. Conclusions

Mechanical properties of commercial castings were investigated by collecting steel specimens from commercial castings, and measuring their tensile test data to determine statistically significant simulation results that correlate with mechanical properties. Sixteen castings from four separate foundries were used in the study. Approximately 190 tensile test specimens machined from blanks cut from the same twelve locations in each casting were analyzed. The measured tensile properties for all foundries are provided here, grouped by casting, along with specimen size tested and summary statistics. The strength data analysis revealed that the data for one foundry was identified to be outliers and lower than all the other foundries. The *UTS* data for this foundry was mostly outside the ranges of all the other foundries. The data from this foundry was excluded from the final analysis of the measured and estimated mechanical property data. The mechanical testing data was analyzed by the specimen ID or location. The measured strength and ductility property data clearly depend on their location in the casting, both in terms of strength values and variability.

The simulation results analyzed for correlations to mechanical properties were the porosity

volume percentage, solidification rate, the Niyama Criterion, the temperature gradient used in Niyama Criterion, the cooling rate used in Niyama Criterion and the cooling rate between 800 °C and 500 °C during the quenching process (*T85*). Data was collected from the gage sections of the specimen locations at ten points to determine a mean and the variation. Points were selected to capture the minimum and maximum values, and at eight representative values at well-spaced. The standard deviation was used as the representative value of the variation of the simulation results. The strength data was observed to have a strong correlation with *T85*. Also a strong correlation for increasing strength with increasing solidification rate was also demonstrated. Above solidification rates of 0.2 °C/s the data showed fairly consistent and high *UTS* properties, above 130 ksi. The porosity predicted in the specimens was fairly low in this study. Nonetheless, a 10 ksi reduction in *UTS,* and a 4 ksi reduction in *YS,* was observed as the predicted porosity increased from a very low level to around 1%.

Strength estimation calculations determined from previous work using casting and heat treatment simulation results were compared with the data measured in the current study. In the previous work, strength estimations for *UTS* and *YS* were determined based on a much smaller set of 18 tensile samples using *T85* and solidification rate simulation results. Using simulation results from the present commercial casting study, the calculated strength data for this study compared well with the measurements, and the standard errors of the calculations are 8.7 and 12.0 ksi for the *UTS* and *YS*, respectively. The estimated properties from simulation results were found to be conservative. The calculated strengths are conservative in the lower range of strength measurements in particular. The measured and estimated property data for the present study were compared to 1% and 10% lower bound properties calculated from a large sample size of SFSA member data (over 1560 data points). It was observed here that all strength property measurements and estimations are above the 1% lower bound. The results of this study support using these lower bound values for *UTS* and *YS* as conservative design properties for commercial castings. The strength estimations presented here were found to give within about 10 ksi accuracy, and they were generally determined to be conservative estimates of the strength variations in 8630 Q&T steel castings.

Acknowledgements

This research is sponsored by the DLA-Troop Support, Philadelphia, PA and the Defense Logistics Agency Information Operations, J62LB, Research & Development, Ft. Belvoir, VA.

References

1. *MAGMAsoft*, MAGMA Gmbh, Kackerstrasse 11, 52072 Aachen, Germany.

2. *Minitab* 21.2 Statistical Software, Minitab, Inc. (www.minitab.com), State College, PA, 2022.

3. *SAS Enterprise Guide* software, Version 8.3 of the SAS System for Windows, SAS Institute Inc., 2020.

4. Poweleit, D., Brown, H., David, D., Hardin, R., Beckermann, C., Foley, R., and Griffin, J., "Establishing Lower Bound Properties for Cast Parts," in Proceedings of the 74th SFSA Technical and Operating Conference, Steel Founders' Society of America, Chicago, IL, 2020.

5. Hardin, R., Beckermann, C., Monroe, R., David, D., and Allyn, B., "Measurements and Predictions of Lower Bound Mechanical Properties of Cast Steels," in Proceedings of the 73rd SFSA Technical and Operating Conference, Paper No. 4.3, Steel Founders' Society of America, Chicago, IL, 2019.